BEST AVAILABLE IMAGES

Defective images within this document are accurate representations of the original documents submitted by the applicant.

Defects in the images may include (but are not limited to):

- BLACK BORDERS
- TEXT CUT OFF AT TOP, BOTTOM OR SIDES
- FADED TEXT
- ILLEGIBLE TEXT
- SKEWED/SLANTED IMAGES
- COLORED PHOTOS
- BLACK OR VERY BLACK AND WHITE DARK PHOTOS
- GRAY SCALE DOCUMENTS

IMAGES ARE BEST AVAILABLE COPY.

As rescanning documents *will not* correct images, please do not report the images to the Image Problem Mailbox.

STIC-ILL

BT - MICROFILM
QP1, A5

From: Chen, Shin-Lin
Sent: Thursday, January 20, 2000 7:34 AM
To: STIC-ILL
Subject: articles

Please provide the following articles by 1-24-00. Thanks!
Serial No. 09/258,217.

1. Bizbiz et al., Atherosclerosis, 1997 (May), 131(1), p. 73-78.

2. Bolobnesi et al., Monaldi Archives for Chest Disease, 1994 (April), 49 (2), 144-149.

3. Maruyama et al., Am. J. Physiol., 1991, 261 (6, pt.2), H1716-H1726.

Ilkiw et al., Circulation Research, 1989 (April), 64 (4), p. 814-825.

Shin-Lin Chen
AU 1633
CM1 12E03
(703)305-1678

Chronic hypoxic pulmonary hypertension in rats and increased elastolytic activity

KAZUO MARUYAMA, CHONGLIANG YE, MICHAEL WOO, HARI VENKATACHARYA, LOIS D. LINES, MEREDITH M. SILVER, AND MARLENE RABINOVITCH
Departments of Cardiology, Pathology, and the Research Institute, The Hospital for Sick Children, and Departments of Pediatrics and Pathology, University of Toronto, Toronto, Ontario M5G 1X8, Canada

MARUYAMA, KAZUO, CHONGLIANG YE, MICHAEL WOO, HARI VENKATACHARYA, LOIS D. LINES, MEREDITH M. SILVER, AND MARLENE RABINOVITCH. *Chronic hypoxic pulmonary hypertension in rats and increased elastolytic activity.* Am. J. Physiol. 261 (Heart Circ. Physiol. 30): H1716–H1726, 1991.— Previously in rats injected with the toxin monocrotaline and administered SC-39026, a serine elastase inhibitor, pulmonary hypertension was decreased in association with reduced muscularization of peripheral pulmonary arteries. To determine whether inhibition of elastolytic activity might prevent this vascular change in other conditions producing pulmonary hypertension, we administered SC-39026 to rats during a 10-day exposure to chronic hypobaric hypoxia. We also measured elastolytic activity in the central pulmonary arteries of rats using [^{3}H]elastin substrate and determined whether there was an increase in activity either as early as 2 days or at completion of the hypoxic exposure, which could be inhibited by SC-39026. To further determine whether the mechanism of muscularization of peripheral arteries is modulated by degradation of elastin or other elastase-susceptible extracellular matrix proteins, we assessed desmosine excretion and ultrastructural alterations in elastin as well as in type IV collagen, fibronectin, and laminin. SC-39026 reduced the number of muscularized arteries and the level of pulmonary arterial pressure during exposure to chronic hypoxia. Elastolytic activity was fourfold higher in central pulmonary arteries 2 days after hypoxia when compared with values in control vessels, and the activity was inhibited by SC-39026. In small peripheral pulmonary arteries there were no significant changes with hypoxia reflected in desmosines or in the immunocytochemistry of elastase-susceptible glycoproteins, with the exception of decreased laminin. This feature was not inhibited by SC-39026. To further assess whether the protective effect of SC-39026 was related to its inhibition of elastase, an extended study was carried out using a different elastase inhibitor, α_1-proteinase inhibitor. An even greater reduction in hypoxia-induced pulmonary hypertension and vascular changes was observed with this elastase inhibitor and the latter included medial hypertrophy.

elastase; elastin; type IV collagen; fibronectin; vascular smooth muscle cell differentiation; protein A-gold; immunoelectron microscopy

CHRONIC HYPOXIA causes pulmonary hypertension and structural changes in the pulmonary vascular bed. These include muscularization of normally nonmuscular arteries and medial hypertrophy of muscular arteries (19–21) associated with an increase in connective tissue proteins, elastin, and collagen (7, 15–17). In rats exposed to chronic hypoxia, Kerr et al. (7) have shown that inhibition of collagen production in the pulmonary artery reduces medial hypertrophy and decreases the level of pulmonary arterial pressure. Although it has been shown that elastin synthesis is increased in the pulmonary artery of calves exposed to chronic hypoxia (15), fragmentation of the internal elastic lamina (17) and partial loss of the endothelial basement membrane (16) have also been observed in these large vessels in rats. This suggests that enzymes that degrade connective tissue proteins may also be important in causing the vascular changes.

In recent studies we have shown that an inhibitor of elastolytic activity decreased muscularization of peripheral normally nonmuscular pulmonary arteries and pulmonary hypertension in rats injected with the toxin monocrotaline. There was, however, no decrease in medial hypertrophy of muscular arteries (6) unless the intravenous analogue SC-37698 was infused continuously (33). We have subsequently related increased elastolytic activity in the central pulmonary arteries to the initiation and the progression of medial hypertrophy in the monocrotaline rat model (L. Todorovich-Hunter, H. Dodo, L. McCready, F. W. Keeley, and M. Rabinovitch, unpublished observations; 29).

Muscularization of normally nonmuscular arteries is ascribed to the differentiation of pericytes to mature smooth muscle cells, and extracellular matrix components are modulators of cell differentiation or phenotype (14). Degradation of matrix components in the pulmonary artery wall by an elastase could induce differentiation of pericytes to smooth muscle cells. We hypothesized that, in the hypoxic as well as the monocrotaline model, degradation of elastin or perhaps some other matrix component such as type IV collagen (12), fibronectin (13), or laminin (4) or proteoglycans (24) by elastolytic activity might lead to differentiation of pericytes to mature smooth muscle cells in normally nonmuscular peripheral pulmonary arteries.

To test this hypothesis, we administered a serine elastase inhibitor SC-39026 (6, 18) to rats during exposure to chronic hypoxia, and we assessed whether this decreased the muscularization of small normally nonmuscular pulmonary arteries as well as the medial hypertrophy of muscular arteries and pulmonary hypertension. To further identify whether, in association with the vascular changes of chronic hypoxia, there was evidence

of elastolytic activity, we counted the number of breaks in the internal elastic lamina and the number of myoendothelial junctions in small muscular arteries. Since changes affecting many small peripheral arteries may be reflected by increased urinary excretion of desmosines (elastin cross-links), this amino acid was measured by Dr. Barry C. Starcher (University of Texas, Tyler, TX). We used immunoelectron microscopy to assess whether in small peripheral nonmuscular arteries the number and distribution of tropoelastin, type IV collagen, fibronectin, and laminin antigenic sites were altered by hypoxic exposure and by administration of the elastase inhibitor, SC-39026. To at least obtain indirect evidence of elastolytic activity in the peripheral arteries, we assessed cross-reactivity with a human neutrophil elastase antibody. We then used a [^{3}H]elastin substrate to measure elastolytic activity in central pulmonary arteries at time points that preceded and were associated with the development of medial hypertrophy, with the view that differences may reflect changes in peripheral vessels where application of the assay was not technically feasible. We also assessed whether the elastolytic activity, if increased, was inhibited in rats administered the elastase inhibitor SC-39026. In addition, we carried out an extended study in which we administered a different elastase inhibitor, α_1-proteinase inhibitor (Prolastin, Cutter Biologicals, Miles, Canada) during exposure to chronic hypoxia and assessed the subsequent effect on the severity of pulmonary hypertension, judged by pulmonary arterial pressure, right ventricular hypertrophy, and pulmonary vascular changes.

MATERIALS AND METHODS

Hemodynamic studies. A neutrophil elastase inhibitor, *dl*-2-chloro-4-(1-hydroxyoctadecyl) benzoic acid (SC-39026), was kindly supplied by Dr. G. Fuller (Searle, Skokie, IL) (18). For the hemodynamic, structural, and ultrastructural studies, 17 male Sprague-Dawley rats weighing 235–300 g were used (Charles River Breeding Laboratories, Ottawa, Ontario, Canada). Each animal was randomly assigned to one of four groups: rats exposed to hypobaric hypoxia for 10 days (air at 380 mmHg) and gavaged with SC-39026 (Hypoxia/SC-I, n = 5); rats exposed to hypobaric hypoxia for 10 days and gavaged with carboxymethylcellulose vehicle (Hypoxia/V, n = 5); room air rats gavaged with SC-39026 (Air/SC-I, n = 3); and room air rats gavaged with vehicle (Air/V, n = 4). The animals gavaged with SC-39026, received twice daily 40 mg/kg of the compound suspended in 0.5 ml 1% carboxymethylcellulose. Carboxymethylcellulose vehicle was prepared by dissolving 1 g of the compound (Sigma, St. Louis, MO) in 100 ml distilled water. Gavage was begun 12 h before the hypoxic exposure period and continued for 10 days, finishing on the morning of the eleventh day. Food and water were provided ad libitum through the duration of hypobaric hypoxia. The rats were removed from the hypobaric chamber twice daily for 15 min each time for the gavage. Six hours after the last gavage, blood samples (1 ml) were obtained under 1.0% halothane anesthesia from the tail vein. The blood was immediately centrifuged and the plasma stored at −70°C for subsequent radioimmunoassay of the level of SC-39026 (carried out by Dr. R. Mueller at Searle, Skokie, IL).

After the hypoxic exposure period, the rats were maintained in room air for 18 h before catheterization to better tolerate the procedure. All rats were first anesthetized with pentobarbital sodium (33 mg/kg) given intraperitoneally. This dose was supplemented as needed during the procedure in increments of 5 mg/kg. The pulmonary artery catheter was Silastic tubing (0.31 mm ID and 0.64 mm OD) and was inserted via a right external jugular vein into the pulmonary artery by a closed-chest technique as previously described (20). Pressures were monitored using a physiological transducer (MS20, Electromedics, Englewood CO), an amplifier system (Interface 4600, Gould, Mississauga, Ontario, Canada), and a monitor (V1000, Gould). The aortic catheter was polyethylene tubing (PE-10, 0.28 mm ID and 0.61 mm OD), and it was inserted into the abdominal aorta under direct vision (19–21). Both catheters were passed under the skin and exteriorized at the back of the rat's neck.

Forty-eight hours after catheterization, i.e., 66 h after removal from hypobaric hypoxia, with the rat fully conscious, pressures were recorded (ES1000, Gould) from both the pulmonary artery and aorta. Blood samples, 0.5 ml each, were obtained from the pulmonary and aortic catheters and Pa_{o_2}, Pa_{co_2}, pH, and oxygen saturations were measured by a blood gas analyzer (Corning Glass Works, Medfield, MA). The hematocrit was determined from an additional 0.1-ml sample. Oxygen consumption was measured as previously described with adjustments for standard pressure and temperature, and cardiac index was calculated (21).

Preparation of lung tissue for structural analysis. After the hemodynamic measurements were completed, the rats were mechanically ventilated (Harvard Rodent Ventilator model 683, S. Natik, MA) through a tracheostomy (tidal volume 3.5 ml, 75 breaths/min) under pentobarbital sodium anesthesia (33–45 mg/kg). A midline sternotomy was performed to expose the heart and lungs. Heparin (1,000 USP/ml) was injected (0.5 ml) into the right ventricular cavity and allowed to circulate for 2 min. The main pulmonary artery was cannulated through a small right ventriculotomy incision with a 5-cm length of polyethylene tubing (PE-205 1.57 mm ID, 2.08 mm OD), which was secured in place with a 2.0 silk suture. The lung was then perfused with preheated (37°C) heparinized (0.5% vol/vol) phosphate-buffered saline (PBS) at 20 cmH_2O pressure to clear the blood, during which time the heart and lungs were removed en bloc while maintaining ventilation. The left pulmonary artery was then temporarily occluded, and the right lung was perfused with fixative (1% glutaraldehyde and 4% formaldehyde in 0.1 M phosphate buffer) at 20 cmH_2O pressure for 10 min. Ten blocks, approximately 1 mm^3, were cut from the midportion of the right lung and placed in the same fixative for 24 h and then processed for transmission electron microscopy, all as previously described (19–21).

The left pulmonary artery was then unclamped, perfused with PBS for 1 min, and injected with a hot (60°C) radiopaque barium-gelatin mixture at 100 cmH_2O pres-

sure for 5 min. The pulmonary artery cannula was clamped and the lung was distended and fixed by perfusion through the tracheal tube with 10% Formalin at 36 cmH_2O pressure for 72 h. A block of tissue 10 × 10 × 5 mm, obtained from the midsection of the left lung, was processed for light microscopy by paraffin embedding. Sections were stained for elastin by the Van Gieson method.

The right ventricle (RV) of the heart was dissected from the left ventricle plus septum (LV + S) and weighed separately. The ratios of RV/(LV + S) and RV (g)/body weight (kg) were calculated.

Light microscopic analysis of pulmonary arteries. Light microscopic slides were analyzed without knowledge of the treatment group. All barium-filled arteries >15 μm external diameter were assessed at 400× (50–85 arteries per rat). Each artery was first identified according to its accompanying airway, as being related to a terminal bronchiolus, respiratory bronchiolus, alveolar duct, or alveolar wall. Each artery was also identified as being one of three structural types: muscular (with a complete medial coat of muscle), partially muscular (with an incomplete coat, only a crescent of muscle being present), or nonmuscular (no muscle apparent). The percentage of muscular and partially muscular arteries at alveolar wall and alveolar duct level was determined. For all the muscular arteries between 50 and 100 μm in diameter (8–17, median 13, were found per section), the wall thickness of the media (distance between external and internal elastic laminae) was measured along the shortest curvature, and a percent wall thickness was calculated (19–21). In each of 10 consecutive fields at 250×, all arteries and alveoli were counted. Arterial density was expressed as the number of arteries per 100 alveoli (19–21).

Transmission electron microscopic analysis of pulmonary arteries. The number of myoendothelial junctions and the number of breaks in the internal elastic lamina were counted in small muscular pulmonary arteries to determine whether there was evidence of elastolytic activity associated with the development of medial hypertrophy 10 days after hypoxic exposure and whether this was altered by SC-39026. Because hemodynamic and light microscopic structural features failed to reveal any significant differences between Air/V and Air/SC-I groups, we combined tissue from both groups in ultrastructural analyses (Air/±SC-I). Tissue blocks were dehydrated and embedded in Epon, and 1-μm sections were cut and stained with toluidine blue. Blocks containing 50–130-μm diameter small muscular pulmonary arteries were chosen, and ultrathin sections (600–900 Å) were cut. The latter were prepared on copper grids, stained with 5% uranyl acetate and 0.4% lead citrate, and viewed in a transmission electron microscope (Philips 201, Philips Electronic Instruments, Mount Vernon, NY). Photomicrographs of the entire circumference of four or five arteries from each group were taken at 2,240× magnification and printed at 17,500× magnification. The number of myoendothelial junctions and the number of breaks in the internal elastic lamina were counted separately (the values were expressed per μm of internal elastic lamina).

Immunocytochemical study of type IV collagen, elastin, fibronectin, laminin, and elastase. An additional nine rats were used in the immunocytochemical studies. For the reasons mentioned above, three groups of rats were studied: Air, Hypoxia, and Hypoxia/SC-I (n = 3 rats per group). The rats were removed from the hypobaric chamber after 4 days, a time-point coincident with significant muscularization of peripheral pulmonary arteries (19). The lung was perfused as previously described for the ultrastructural studies, but the fixative was 0.1% glutaraldehyde and 4% formaldehyde in 0.1 M phosphate buffer. Blocks (~1 mm^3) were cut from the midportion of the right lung and placed in the same fixative for 2 h and then embedded in Lowicryl K4M at 4°C (26). The right lower lobe was removed after perfusion with buffer, frozen in liquid nitrogen, and 5-μm sections were subsequently prepared to determine whether there was cross-reactivity with human neutrophil elastase antibody, since an antibody to rat vascular elastase is not available.

From Lowicryl-embedded tissue, 1-μm sections were cut and stained with toluidine blue, and those that included 20–40 μm small nonmuscular pulmonary arteries were chosen for ultrathin sections. To localize tropoelastin, type IV collagen, fibronectin, and laminin, a protein A-gold immunocytochemical postembedding technique was applied (26). Thin sections of arteries from all three rat groups, Air, Hypoxia, Hypoxia/SC-I, were labeled simultaneously with each antibody. Thin sections on nickel grids were incubated for 30 min in 3% bovine serum albumin, essentially globulin free (Sigma, St. Louis, MO), to block nonspecific binding of protein. The sections were then, without rinsing, incubated overnight at 4°C in one of the following: a 1:100 dilution of rabbit antibody raised against bovine tropoelastin (kindly supplied by Dr. Robert P. Mecham, Washington University, St. Louis, MO); a 1:4,000 dilution of affinity purified goat antibody raised against human and bovine type IV collagen (Southern Biotechnology Associates, Birmingham, AL); a 1:100 dilution of rabbit antibody raised against human fibronectin (Chemicon International, El Segundo, CA); or a 1:100 dilution of rabbit polyclonal antibody raised against mouse laminin (Collaborative Research, S. Natik, MA). The sections for type IV collagen were followed by 1-h incubation with 1:3,000 rabbit anti-goat immunoglobulin antibody (Dako, Denmark) applied directly to the grid. After being jet rinsed with PBS, the sections were incubated for 1 h at room temperature on drops of protein A-gold (grain size 20 nm). The sections were jet rinsed with distilled water and air dried before being counterstained with uranyl acetate and lead citrate. The specificity of the immunolabeling was assessed by substituting PBS for the primary antibody and by free protein A before protein A-gold (26). We ascertained that the degree of nonspecific labeling was minimal and similar to the "background level" described below (i.e., the number of counts/μm^2 over nuclei and air spaces). Immunofluorescence on rat lung frozen sections and immunogold labeling as described above were carried out using human neutrophil elastase antibody (kindly supplied by Dr. Robert P. Mecham), but it did not cross-react with rat pulmonary arterial wall elastase.

For each animal, 1–4 small 20- to 40-μm external diameter nonmuscular pulmonary arteries (Table 3) were photographed at 3,200× and printed at 25,000× magnification (Philips 201, Philips Electronic Instruments, Mount Vernon, NY). Photomicrographs were developed, and the negatives were analyzed using a semiautomatic computerized system (Interactive Image Analysis System IBAS-1, Zeiss, Thornwood, NY). The distribution of tropoelastin, type IV collagen, fibronectin, and laminin antigenic sites was compared, and the effect of hypoxic exposure (±SC-39026) was assessed. The number of gold particles reflecting tropoelastin and type IV collagen and laminin antigenic sites were counted on separate photomicrographs and related to the surface area of the adjacent or underlying single elastic lamina, planimeterized, and calculated by the IBAS-1 image analyzer. The number of gold particles on air spaces and nuclei were also counted and calculated (per μm^2) as "background values." The background values, e.g., 0.84 ± 0.10 (SE) particles/μm^2, 0.92 ± 0.07 particles/μm^2, and 1.51 ± 0.1 particles/μm^2, for tropoelastin, type IV collagen, and laminin antigenic sites, respectively, were then subtracted from the totals to calculate the number of particles per surface area. Fibronectin antigenic sites were observed largely in the regions between endothelial cells and pericytes thus making quantitative evaluation more problematic and therefore qualitative assessment only was carried out.

Measurement of urine desmosine levels. An additional 12 rats were used for measurement of desmosine in the urine (3, 11). As in the immunocytochemical studies, three groups of rats ($n = 4$ in each) were studied: Air, Hypoxia, and Hypoxia/SC-I. The rats were placed in metabolic cages for an initial 24-h baseline period in room air, and urine was collected. The animals were then placed in room air or hypoxia, and urine was again collected after every 24-h period for up to 4 days. Each time, the bottom of the cage was rinsed with about 100 ml of distilled water, which were then added to the total volume of urine. This diluted urine was immediately centrifuged, the volume of the supernatant was measured, and the supernatant was then stored at −20°C until the time of assay. Urine creatinine was determined using the Creatinine Analyzer 2 (Beckman, Fullerton, CA). To assay desmosine, the urine was hydrolyzed in 6 N HCl, the acid was then evaporated, and the hydrolysate was dissolved in assay buffer. Quantitation of desmosine was performed by radioimmunoassay as previously described (3, 11). The results of urine desmosine levels were described as a ratio of total desmosine to total creatinine [desmosine (pM)/creatinine (mg)].

Assay of elastolytic activity. An assay for elastolytic activity originally described by Hornebeck et. al (4) and modified by our group (8) was used. Central pulmonary arteries from hypoxia-exposed and room air rats were assayed together, and comparisons were made at the 2-day and 10-day time points. For each assay, pooled tissue from eight rats was used, and determinations of elastase activity were carried out in triplicate. Each assay was repeated three times at the 2-day and 10-day time points. Purified elastin was radiolabeled using [^{3}H]$NaBH_4$ (sp act 319 mCi/mmol, New England Nuclear, Boston, MA) and the [^{3}H]elastin substrate (sp act 2,126 cpm/μg elastin) used was a gift from Dr. Robert Senior and Gail Griffin, (Washington University, St. Louis, MO).

The rats used were weight matched to those in the previous experiments and similarly randomly assigned to hypoxia or normoxia groups. To prepare the pulmonary artery tissue for assay, rats were killed and exsanguinated using a guillotine. All dissections were done as rapidly as possible, taking ~20 min per rat. A midline sternotomy provided access to the central pulmonary artery and both right and left branches. The pulmonary artery was cannulated via the right ventricle, and both branches were probed to the hilum of each lung, cleared of debris, and then removed. The vessels were further cleaned of all adhering fat, blood, and loose connective tissues, weighed, washed with 1 ml of physiological saline (0.9% NaCl), vortexed, and then centrifuged at 1,500 *g* for 3 min at 4°C at least three times or until the supernatant was colorless. The pulmonary arteries were then finely minced with a razor blade and centrifuged at 1,500 *g* for 5 min at 4°C, at least three times or until the supernatant was colorless, i.e., blood was no longer apparent. Tissue from eight pulmonary arteries was pooled, 500 μl 0.9% NaCl was added, and the mixture was homogenized twice for 1.5 min on ice using a Polytron set at 10,000 rpm. The homogenates were centrifuged at 2,800 *g* for 30 min at 4°C, the supernatants were discarded, and the pellet was used as the source of elastase. (In pilot studies, no elastolytic activity was found in the supernatants.)

Extraction of elastolytic activity was carried out by adding 1 ml of 0.5 M Na acetate buffer, pH 4.0, and 0.02% wt/vol sodium azide to the tissue pellet. The solution was mixed constantly overnight at 4°C then microcentrifuged at 10,000 *g* for 30 min at 4°C. The supernatant was collected and stored at −70°C until needed, and the pellets were reextracted. The extracts were pooled, dialyzed against distilled H_2O overnight at 4°C, and then lyophilized. To precipitate elastase, a solution of 60% saturated ammonium sulfate was added to the lyophilized tissue extract in an end volume of 500 μl. The suspension was stirred for 1 h at room temperature, placed at 4°C overnight, then microcentrifuged at 8,160 *g* for 1 h at 4°C. The supernatant was discarded and the protein pellet resuspended, on ice, in 300 μl of 50 mM tris(hydroxymethyl)aminomethane (Tris)-HCl assay buffer, pH 8.0, containing 150 mM NaCl, 10 mM $CaCl_2$, 0.02% polyoxyethylene 23 lauryl ether (Brij) and 0.02% NaN_3.

To each Eppendorf assay vial, 20 μl of the substrate [^{3}H]elastin and 40 μl of the tissue sample were added, and the volume was adjusted to 220 μl with Tris assay buffer. The samples were vortexed, incubated at 37°C for 18 h, then microcentrifuged for 4 min at 8,160 *g*; 100-μl aliquots of the supernatant containing solubilized [^{3}H]-elastin fragments were mixed with 4 ml of ACS scintillation fluid and counted for 2 min (LKB, Wallac 1219 Rackbeta counter, San Francisco, CA). Human leukocyte elastase (HLE) (Elastin Products, Pacific, MO) standards in dilutions of 2.5–0.0375 ng, were also run with each tissue assay. To further characterize the elastase activity, inhibitors (10 μl) were preincubated with the tissue samples for 0.5 h at 37°C before adding the sub-

strate. The inhibitors used were 2 mM phenylmethylsulfonyl fluoride (PMSF), 50 μM SC-39026, both serine-proteinase inhibitors, and 2 mM Na_2EDTA, a metallo-proteinase inhibitor. The doses were chosen according to previously published reports (9) and *Pseudomonas aeruginosa* elastase (Elastin Products, St. Louis, MO) was used as a positive control for EDTA.

We added 2 mM *N*-methylamine to all solutions to bind α_2-macroglobulin. The latter is a potent elastase inhibitor normally bound to vascular endothelial cells. Our concern was that homogenizing the vessel would allow α_2-macroglobulin to bind elastase and effectively reduce the activity measurable in the assay. We also used polypropylene tubes and transferred solutions with polypropylene pipette tips, since elastase absorbs onto glass. Because of the results of our study, assays were subsequently carried out in triplicate in groups of eight control and eight hypoxia rats at the 2-, 4-, 8-, 10-, and 14-day time points and only in rats administered SC-39026 during hypoxia at the 2-day time point. The tissue was harvested 4–5 h after the last dose. The latter time point was chosen based on the pharmacokinetics of SC-39026 as previously established (18).

Studies with α_1-proteinase inhibitor. To further confirm that any protective effect of SC-39026 on hypoxic pulmonary hypertension was, in fact, related to inhibition of elastolytic activity, we carried out similar experiments with a different elastase inhibitor, α_1-proteinase inhibitor (Prolastin, kindly supplied by Mary Ann Lark and Stan Beck of Cutter Biologicals, Miles, and Etobicoke, Ontario, Canada). This compound (A_1-PI) was given intravenously by an initial 200 mg/kg bolus and subsequent osmopump infusion of 120 $mg \cdot kg^{-1} \cdot day^{-1}$ beginning 12 h before exposure to hypoxia or normoxia. This dose was based on previous experimental studies in the literature (2) and our own pilot work in which lower doses were initially tried but proved ineffective (data not shown). The osmopump (Alzet 2ml1, Alza, Palo Alto, CA) was primed by overnight incubation in 0.9% NaCl and implanted under pentobarbital anesthesia as previously described (21). Briefly, a catheter was first inserted into the left jugular vein and tunneled subcutaneously to the base of the skull where it was attached to the delivery port of the osmopump, which was then implanted at the back of the neck. The osmopumps were replaced with new fully primed pumps at 7 days and continued to infuse through the remaining 3 days of hypoxia and the time in normoxia until killed. We compared five rats infused with A_1-PI in hypoxia to three vehicle-infused hypoxia rats and three vehicle-infused room air control rats with respect to body weights, pulmonary and aortic pressures, right ventricular weights, and light microscopic morphometric analysis of the pulmonary arteries of the lung using the techniques and endpoints (extension of muscle, medial hypertrophy, and number of barium-filled arteries) previously described in this study. Only three room air/vehicle and three hypoxia/vehicle rats were chosen for these experiments, since the findings were in keeping with the previously studied rats from these groups in the SC-39026 study.

Statistical analysis. The data were expressed as means ± SE. For hemodynamic and light microscopic studies, data were analyzed statistically by a two-way analysis of variance to assess the effect of hypoxia and SC-39026 treatment. Duncan's test of multiple comparisons was then used to establish which groups were different. Linear regression analysis was used to detect whether, in individual hypoxic rats gavaged with SC-39026, there were correlations between the level of mean pulmonary arterial pressure and the severity of structural abnormality in the pulmonary arteries and the plasma SC-39026 levels. For transmission and immunocytochemical electron microscopic studies and the urine desmosine study, one-way analysis of variance (ANOVA) was used followed by Duncan's test of multiple comparisons when significant differences were found. One-way ANOVA followed by Tukey's test of multiple comparisons was used to assess differences in elastolytic activity between hypoxia and normoxia rats and hypoxia + SC-39026 rats at the 2-day time point and also to assess differences between the three groups in the A_1-PI study. Differences were considered statistically significant at $P < 0.05$.

RESULTS

Weight gain, hemodynamic assessments and right ventricular hypertrophy. Rats exposed to hypoxia lost weight during the first 7 days, but then they began to gain weight, whereas rats kept in room air gained weight steadily. Thus final body weights in hypoxia-exposed rats were ~80% of those room air rats ($P < 0.01$, ANOVA) (Table 1). SC-39026 had no significant effect on body weight in either group. Exposure to hypoxia also resulted in an increase in hematocrit ($P < 0.01$, ANOVA); a change unaffected by SC-39026 (Table 1). There were no significant differences in mean aortic pressure, cardiac output, and arterial blood gases among the four groups (Tables 1 and 2).

All rats gavaged with SC-39026 had plasma levels ranging from 1.43 to 3.71 μg/ml. These values are considered in the therapeutic range (Searle Research and Development) and are comparable to those achieved in previous studies (6) (Table 2). Values in room air and hypoxia rats were similar. In both room air and hypoxia rats gavaged with vehicle only, plasma level values of SC-39026 were 0.04–0.29 μg/ml, in keeping with background activity for the assay.

Mean pulmonary arterial pressure. Exposure to 10 days of hypoxia caused significant pulmonary hypertension ($P < 0.01$, ANOVA) (Fig. 1). The mean pulmonary arterial pressure values of the room air rats gavaged with vehicle (Air/V) and SC-39026 (Air/SC-I) were 17.0 ± 1.2 and 18.3 ± 1.5 mmHg, respectively. Hypoxia/V rats had values of 33.4 ± 1.2 mmHg, whereas in Hypoxia/SC-I rats, there was a slight but significant reduction to 29.0 ± 1.1 mmHg ($P < 0.05$). There was no significant correlation between the reduction in pulmonary arterial pressure and the plasma SC-39026 level.

Right ventricular hypertrophy. Hypoxic exposure caused significant right ventricular hypertrophy (Table 2). This was evident both by an increased ratio of RV/(LV + S) and RV/body weight ($P < 0.01$ for both, ANOVA). SC-39026 had no effect on the development of right ventricular hypertrophy.

TABLE 1. *Body weight, hematocrit, and arterial blood gases*

	n	Weight, g			Hematocrit, %	pH	Pa_{O_2}, mmHg	Pa_{CO_2}, mmHg
		Initial	7 Days	Final				
Air/V	4	275±10	302±14	311±14	43±1	7.46±0.02	81±5	37±2
Air/SC-I	3	291±6	328±6	333±7	41±1	7.41±0.03	80±8	39±3
Hypoxia/V	5	290±4	253±4*	265±6*	56±1*	7.45±0.01	79±2	36±2
Hypoxia/SC-I	5	277±11	242±9*	253±10*	55±1*	7.46±0.01	82±2	40±1

Values are means ± SE; *n*, number of rats. Final, body weights at the time of hemodynamic measurements, i.e., 10 days of hypoxic/normoxia + 2 days after cardiac catheter placements; Air/V, room air rats gavaged with vehicle; Air/SC-I, room air rats gavaged with SC-39026; Hypoxia/V, rats exposed to hypoxia and gavaged with vehicle; Hypoxia/SC-I, rats exposed to hypoxia and gavaged with SC-39026; Pa_{O_2} and Pa_{CO_2} arterial O_2 and CO_2 tensions, respectively. Blood gases were measured as described in MATERIALS AND METHODS with the animals anesthetized just before being killed. *$P < 0.01$ compared with Air groups (ANOVA).

TABLE 2. *Hemodynamic measurements, structural assessments, and plasma SC-39026 levels*

	n	Mean Aortic Pressure, mmHg	Cardiac Index, $ml \cdot kg^{-1} \cdot min^{-1}$	O_2 Cons, $ml \cdot kg^{-1} \cdot min^{-1}$	RV/(LV + S)	RV/BW, g/kg	Plasma SC-39026 Levels, μg/ml	% Medial Wall Thickness, %	Arteries/ 100 Alveoli
Air/V	4	109±5	459±65	30.4±1.4	0.25±0.01	0.48±0.01	0.15±0.05	2.9±0.5	3.3±0.2
Air/SC-I	3	105±5	460±66	32.8±1.6	0.24±0.01	0.48±0.01	2.92±0.74‡	2.6±0.6	3.8±0.2
Hypoxia/V	5	111±5	517±41	28±2.3	0.41±0.04†	0.79±0.1†	0.13±0.26	5.8±0.5*	2.5±0.4*
Hypoxia/SC-I	5	112±5	513±64	24±1.2	0.41±0.02†	0.86±0.06†	2.20±0.26‡	5.6±0.9*	2.1±0.3*

Values are means ± SE; *n* = number of rats. RV, right ventricle; LV + S, left ventricle + septum; BW, body weight. For other definitions, see Table 1. Values for cardiac index are based on O_2 consumption (O_2 Cons). * $P < 0.01$ compared with Air groups (ANOVA); † $P < 0.01$ compared with Air groups (ANOVA); ‡ $P < 0.01$ compared with vehicle groups (ANOVA).

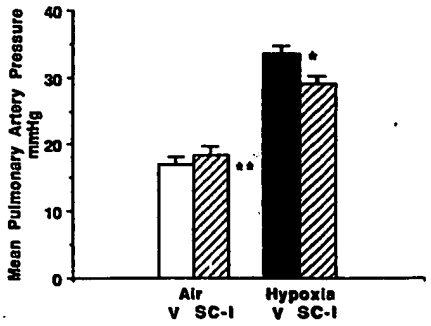

FIG. 1. Mean pulmonary arterial pressure values in 4 groups. Hypoxia groups have significantly higher values than Air groups, **$P < 0.0001$ (ANOVA) but Hypoxia/SC-I group was significantly lower than Hypoxia/V group, *$P < 0.05$ (Duncan's multiple range test). V, vehicle; SC-I, elastase inhibitor (SC-39026). Air/V, $n = 4$; Air/SC-I, $n = 3$; Hypoxia/V, $n = 5$; Hypoxia/SC-I, $n = 5$. Values are means ± SE.

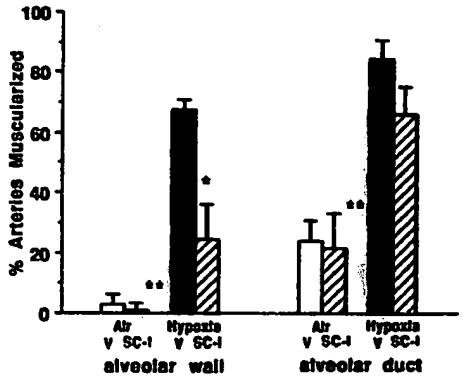

FIG. 2. Percentage of muscularized arteries at alveolar wall and duct level. Hypoxia groups had abnormally increased muscularization of arteries at alveolar wall and alveolar duct level compared with Air groups, **$P < 0.0001$ (ANOVA). Hypoxia/SC-I group compared with Hypoxia/V group had decreased muscularization at alveolar wall level, *$P < 0.05$ (Duncan's multiple range test) with a similar trend at alveolar duct level, although not statistically significant. See Fig. 1 for abbreviations and *n* values. Values are means ± SE.

Vascular changes on light microscopy. Hypoxia increased the percentage of muscular and partially muscular arteries in normally nonmuscular arteries at both alveolar wall and alveolar duct level ($P < 0.01$ for both, ANOVA) (Table 2, Fig. 2). There were ~3% alveolar wall arteries and ~25% alveolar duct arteries muscularized in Air/V rats and similar values in Air/SC-I rats (Fig. 2). Hypoxia/V rats had ~63% alveolar wall and ~84% alveolar duct arteries muscularized. Hypoxia/SC-I rats had a decrease in muscularization of alveolar wall arteries of ~25% ($P < 0.05$), and there was a trend toward a reduction at alveolar duct level as well, but values did not reach statistical significance.

Hypoxia increased the percent wall thickness of small normally muscular arteries assessed, i.e., those between 50 and 100 μm external diameter ($P < 0.01$, ANOVA) (Table 2). SC-39026 had no effect on the increase in percent wall thickness induced by hypoxia (Table 2). There was a decrease in the number of barium-filled arteries per 100 alveoli in hypoxia rats ($P < 0.01$, ANOVA), a feature also unaffected by SC-39026.

Transmission electron microscopic analysis of small muscular arteries. In small muscular arteries (50–130 μm in diam) after 10 days of hypoxic exposure, no significant changes were observed in either the number of the myoendothelial junctions and contacts or in the number of breaks in the continuity of the internal elastic lamina (Table 3), which could suggest ongoing elastin degradation. The numbers of myoendothelial junctions were few (1–3/vessel) but remarkably consistent per 100 μm, whereas the number of breaks was higher (40–60/100 μm).

Immunocytochemical studies in nonmuscular arteries.

TABLE 3. *Morphometric assessment by transmission electron microscopy and immunoelectron microscopy*

	Transmission Electron Microscopy: Small Muscular Arteries (50–130 μm)				Immunoelectron Microscopy: Nonmuscular Arteries (20–40 μm)					
	n	No. of myoendothelial junctions/μm	No. of breaks of internal elastic lamina/μm		*n*	Tropoelastin antigenic sites/μm²	*n*	Type IV collagen antigenic sites/μm²	*n*	Laminin antigenic sites/μm²
Air/±SC-I	5	0.017±0.006	0.46±0.08	Air	7	34.4±1.8	11	4.37±0.59	5	27.31±0.38*
Hypoxia/V	5	0.017±0.007	0.58±0.11	Hypoxia	5	28.5±3.0	7	4.23±0.86	9	21.96±1.30
Hypoxia/SC-I	4	0.021±0.006	0.46±0.07	Hypoxia/SC-I	5	29.3±1.2	6	6.18±0.69	4	20.21±2.70

Values are means ± SE; *n* = number of arteries from each group. In small muscular arteries (50–130 μm) studied by transmission electron microscopy, Air/±SC-I group includes room air rats with and without SC-39026, and Hypoxia/V group was rats exposed to hypoxia and gavaged with vehicle; in peripheral nonmuscular arteries (20–40 μm) studied by immunoelectron microscopy the Air group was not given SC-39026 or vehicle, and the Hypoxia group was not given vehicle. * $P < 0.05$ from groups below.

Protein A-gold particles reflecting tropoelastin antigenic sites were observed throughout the single elastic lamina (Fig. 3), whereas those for type IV collagen and laminin were found along the cytoplasmic membranes of cells along the edge of the internal elastic lamina. On the other hand, fibronectin antigenic sites were located mainly along the "junctional area" between endothelial cells and pericytes (Fig. 4). Hypoxia induced no significant changes in the number (Table 3) or in the distribution of gold-labeled antigenic sites for fibronectin, collagen IV, or fibronectin, but there was a significant decrease in laminin, a feature unaffected by SC-39026 (Table 3).

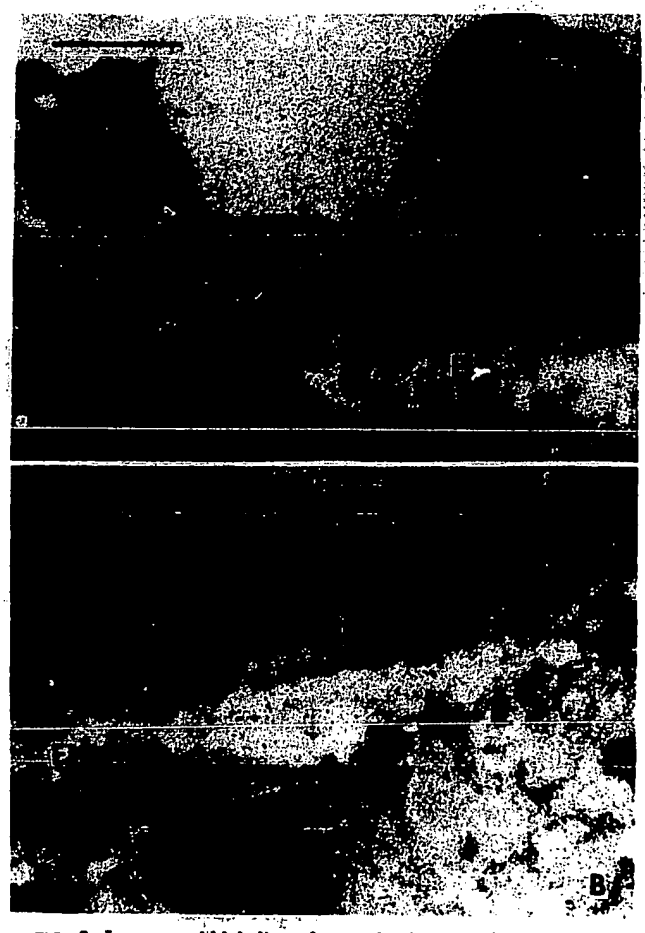

FIG. 3. Immunogold labeling of tropoelastin in single elastic lamina in normally nonmuscular arteries. *A*: immunogold labeling of tropoelastin in normally nonmuscular artery in a room air rat; *B*: 4 days of hypoxic exposure in a rat. Tropoelastin antigenic sites are localized throughout lamina. There are no significant differences in quantity (see Table 3) and distribution between room air and hypoxic rats. End, endothelium; Peri, pericyte; EL, elastic lamina; arrow, gold particles demonstrating antigenic sites. Bar = 1 μm.

Urine desmosine levels. Since urinary desmosine values can be quite variable (11), we used each animal as its own control. There were no differences among the groups in the average or peak desmosine excreted in the urine when comparing the baseline value and subsequent 4-day room air or hypoxia exposure period (Table 4).

Elastolytic activity. There was a four to ninefold increase in elastolytic activity expressed per segment or per milligram tissue in pulmonary arteries from rats after 2 days of hypoxia compared with values from normoxia controls. At 10 days after exposure, values were not significantly different when expressed per segment pulmonary artery or per milligram pulmonary artery tissue when compared with normoxia controls. Elastolytic activity was inhibited by SC-39026 and PMSF but not by EDTA, confirming that it was a serine proteinase. In rats gavaged during 2 days of hypoxia with SC-39026, pulmonary artery elastolytic activity was reduced by 50%, but values were still higher than in control rats. In other evaluated time points, there was a persistent increase in elastolytic activity at 4 days of hypoxic exposure but no increase at 8 or 14 days (data not shown).

α_1-Proteinase inhibitor. Treatment with A_1-PI during hypoxia was associated with a reduced level of pulmonary arterial pressure of 24 ± 2 mmHg compared with 34 ± 1 mmHg in Hypoxia-V rats ($P < 0.01$, Table 5). Pulmonary arterial pressure values in hypoxia/A_1-PI rats were slightly but not significantly higher that those in Air/V rats (19 ± 2 mmHg). Associated with the reduced pulmonary hypertension in Hypoxia/A_1-PI relative to Hypoxia/V rats, right ventricular hypertrophy was less ($P < 0.05$), as were the extension of muscle into peripheral arteries and medial hypertrophy of muscular arteries ($P < 0.01$ for both comparisons), and there was a slight but significant improvement in the number of barium-filled arteries seen ($P < 0.05$). Pulmonary vascular abnormalities and right ventricular hypertrophy were still apparent in Hypoxia/A_1-PI relative to room air rats ($P < 0.05$ for each comparison), although less than in Hypoxia/V rats.

DISCUSSION

SC-39026 when administered to rats by gavage during a 10-day exposure to hypoxia results in a slight but

FIG. 4. Immunogold labeling of fibronectin in normally nonmuscular arteries. *A*: immunogold labeling of fibronectin in a normally nonmuscular artery in a room air rat; *B*: 4 days of hypoxic exposure in a rat. Fibronectin antigenic sites are located mainly along "junctional area" between endothelial cells and pericytes. Hypoxia induced no significant changes in distribution of fibronectin. Elastic lamina appears to be split along the process of pericyte but was not continuous around vessel wall as a double lamina. See Fig. 3 for abbreviations. Bar = 1 μm.

significant decrease in the severity of pulmonary hypertension associated with a more marked reduction in the number of peripheral arteries muscularized at alveolar wall level. This is likely a reflection of the fact that other factors that contribute to the elevation in pulmonary vascular resistance such as hematocrit were not reduced by administration of the elastase inhibitor. There is, however, no significant effect of SC-39026 on medial wall thickness of the more proximal muscular arteries or on right ventricular hypertrophy. Transmission and immunoelectron microscopic studies and desmosine levels did not provide evidence of degradation of elastin or other extracellular matrix proteins before or coincident with morphologic evidence of smooth muscle differentiation and hypertrophy. Elastolytic activity determined in central pulmonary arteries was, however, higher in vessels of rats after only 2-day exposure to chronic hypoxia but returned to control values by 8 days. We also confirmed that increased elastolytic activity measured in large central pulmonary arteries was less in rats treated with SC-39026.

Urinary desmosine levels were not increased in association with the increase in pulmonary artery elastolytic activity, but this may mean that the degraded elastin remained in the vessel wall as has been shown in other studies (27) or that the increase contributed little to overall elastin synthesis/degradation balance from other organs, e.g., skin, etc. In extended studies where we infused a different elastase inhibitor α_1-proteinase inhibitor (A_1-PI) in rats during exposure to chronic hypoxia, we reduced pulmonary hypertension, and the latter agent and/or method of administration appeared even more effective judged by further reduction in pulmonary arterial pressure, right ventricular hypertrophy, and vascular changes, including extension of muscle into peripheral arteries, as well as medial hypertrophy of muscular arteries. We also achieved slightly less reduction in the number of barium-filled arteries. This feature, the reduced number of barium-filled peripheral pulmonary arteries associated with exposure to hypoxia, has been reported previously by our group (19–21). While we do not know the mechanism, it may reflect resorption of partially occluded arteries as has been described in the rabbit ear chamber (25). It is possible that this is also a response associated with degradation of extracellular matrix components. Alternatively, this may reflect the presence of peripheral arteries partially occluded by swollen endothelial cells that do not fill with barium and are more difficult to appreciate.

In the monocrotaline model of pulmonary hypertension, structural changes precede the development of pulmonary hypertension (23), whereas in the hypoxic model, pulmonary vasoconstriction precedes the vascular abnormalities (20, 21). Despite the differences in etiology, the vascular changes (i.e., medial hypertrophy of normally muscular arteries and abnormal muscularization of nor-

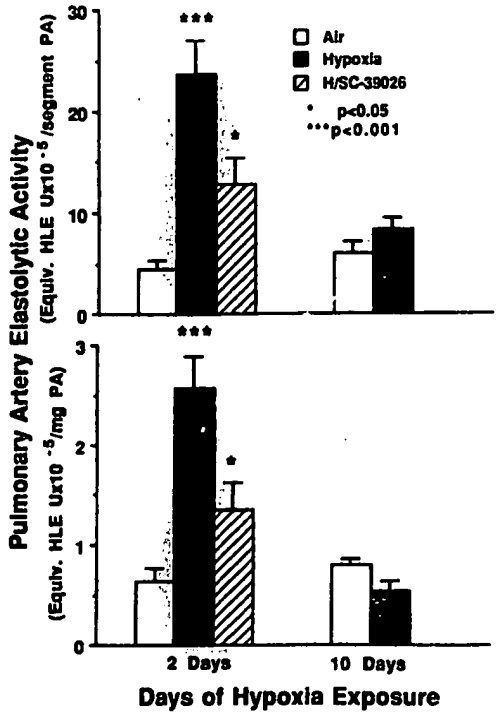

FIG. 5. Elastolytic activity in central pulmonary arteries after hypoxia exposure. Elastolytic activity expressed per pulmonary artery segment (seg/PA) as units (U) of human neutrophil (leukocyte) elastase (HLE) standard. Values from vessels of room air rats are denoted by open bars and values from vessels of hypoxia rats by solid bars. Triplicate assessments were made from 8 pooled pulmonary arteries at each time point, and assays were repeated 3 times at the 2-day and twice at the 10-day time point. Bars are means ± SE from 9 values at 2 days and from 6 values at 10 days. There were 3 values obtained from pooled arteries from 8 SC-39026 (SC-I)-treated hypoxia rats (hatched bar). Significantly higher elastolytic activity is evident in vessels from rats after 2 days of hypoxia when compared with normoxia controls (***$P < 0.001$), but values are significantly reduced in hypoxia SC-I rats (*$P < 0.05$). Values from hypoxia and normoxia rats at 10 days are similar to 2-day controls.

TABLE 4. *Urine desmosine levels*

	Day				
	1	2	3	4	5
Air	341±61	456±50*	377±77*	498±46	391±114
Hypoxia	829±251	677±107	690±143	628±195	706±164
Hypoxia/SC-I	654†	949±74	638±86	564±52	604±48

Values are means ± SE of 4 values (n). * mean of 2 values; † mean ± SE of 3 values. Technical difficulties precluded assay of some specimens. *Day 1* is baseline, *days 2–5* represent air or hypoxia exposure. Units are in pM desmosine/mg creatinine.

mally nonmuscular arteries) are similar. In both models, abnormal muscularization of alveolar wall arteries was significantly reduced by SC-39026 (6), suggesting a common mechanism at the cellular level.

In normally nonmuscular small arteries, pericytes are located in the subendothelium (17). The function of pericytes remains unclear, but they appear to differentiate normally to mature smooth muscle cells as the vessel grows in size (17) and abnormally in all conditions producing pulmonary hypertension. This results in a medial layer of smooth muscle in previously nonmuscular peripheral arteries (mostly <50 μm, 17). On the other hand, the increase in medial wall thickness, which is measured in more proximal normally muscular arteries, i.e., ≥50 μm, reflects hypertrophy and hyperplasia of preexisting smooth muscle cells. Both in monocrotaline and hypoxia-induced pulmonary hypertension models, SC-39026 did not reduce the medial hypertrophy of normally muscular arteries, despite the fact that elastolytic activity was increased in the large central pulmonary arteries as early as 2 days after exposure to hypoxia and at a similar time point after injection of monocrotaline (28). However, the activity measured in the tissue is inhibited by SC-39026. This suggests that a higher dose or more constant level of elastase inhibitor may be necessary to prevent medial hypertrophy, and this is supported by more recent studies in our laboratory in monocrotaline-injected rats and in which we have shown that SC-37698, the intravenous analogue of SC-39026 (33), effectively reduces medial hypertrophy. It is also supported by the fact that a different elastase inhibitor (A_1-PI) given intravenously at high dose results in a reduction in medial hypertrophy. With A_1-PI there is a more impressive reduction in the level of pulmonary arterial pressure in keeping with the more effective inhibition of structural changes with elastase inhibitors, especially the severity of extension of muscle into peripheral arteries.

Both abnormal "extension" of smooth muscle into distal vessels and medial hypertrophy of proximal muscular pulmonary arteries during hypoxia are caused by altered flow and pressure rather than by the direct effect of low oxygen tension (20). It is conceivable that the increase in pressure or in stress on the endothelial cell or directly on the pericyte or smooth muscle cell results in the production of a mediator that induces differentiation or hypertrophy. It has been shown that enzymes with elastolytic activity degrade the extracellular matrix, and this could induce changes in cell phenotype (14). The increased central pulmonary artery elastolytic activity, which we documented just 2 days after exposure to hypoxia, may also occur in intrapulmonary vessels and if so, would support this enzyme's involvement in the pathogenesis of pulmonary vascular changes that occur early after exposure to chronic hypoxia. Unfortunately, given the present methodology, it is not possible to measure elastolytic activity immunochemically or biochemically in peripheral vessels. It is therefore entirely possible that the mechanism of muscularization of peripheral arteries is unrelated to elastolytic activity and that SC-39026 is having some other effect on small arteries related to the inhibition of differentiation of muscle from precursor cells.

Indirect assessments of elastolytic activity in small arteries using morphometric electron and immunoelectron microscopy and desmosine levels were negative. Because neutrophil elastase degrades the cross-linked region of elastin (32), elastase might actually expose more tropoelastin antigenic sites, but we saw neither an increase nor a decrease in chronically hypoxic rats. Proteolytically damaged elastin may be reincorporated into intact elastin during the repair process (27). If this happens in the chronic hypoxic model, there may not be a change in the number of tropoelastin antigenic sites nor an increase in desmosine in urine, because damaged

TABLE 5. *Body weight, hemodynamic measurements, and structural assessments*

	n	Weight, g		Mean Pulmonary Arterial Pressure, mmHg	Mean Aortic Pressure, mmHg	RV/(LV + S)	Medial Wall Thickness, %	Muscular Arteries Alveoli, %		Arteries/100 Alveoli
		Initial	Final					Duct	Wall	
Air/V	3	259±5	314±6	19±2	110±6	0.30±0.02	2.6±0.6	30±0.5	4±0.1	5.4±0.3
Hypoxia/V	3	267±4	244±0.3*	34±1	103±3	0.55±0.06*	5.4±0.7*	90±2.1*	59±2.7*	2.3±0.1*
Hypoxia/A_1-PI	5	262±5	225±10*	24±2‡	108±4	0.40±0.04†§	4.2±0.9‡§	62±1.7‡§	29±1.5‡§	2.9±0.2‡§

Values are means ± SE; n = number of rats. Initial, weight run to exposure; Final, weight at the time of hemodynamic assessment, i.e., after 10 days of hypoxia/normoxia exposure and 2 days after cardiac catheter placement; Air/V, room air rats infused with vehicle; Hypoxia/V, rats exposed to hypoxia and infused with vehicle; Hypoxia/A_1-PI, rats exposed to hypoxia and infused with A_1-PI. A_1-PI: α_1-proteinase inhibitor (Prolastin, Cutter Biologicals, Miles, Canada). * $P < 0.01$ compared with Air/Vehicle group (ANOVA); † $P < 0.05$ compared with Hypoxia/Vehicle group (ANOVA); ‡ $P < 0.01$ compared with Hypoxia/Vehicle group (ANOVA); § $P < 0.05$ compared with Air/Vehicle group (ANOVA).

elastin remains in the vessel wall. If elastase was inducing pericyte differentiation to smooth muscle cells by degrading type IV collagen, fibronectin, or laminin, we would have expected to see a decrease in the number or at least an alteration in the distribution of antigenic sites. The only difference observed, namely the decrease in laminin sites with hypoxia, was not influenced by SC-39026 administration. Since we specifically evaluated nonmuscular peripheral arteries, it is possible that the changes in matrix proteins were occurring early and had vanished even before there was morphological evidence of cell differentiation or that the number of vessels examined and the time points chosen were not sensitive enough as endpoints.

Fragmentation of the internal elastic lamina of the hypertrophied large hilar pulmonary artery has been observed qualitatively in rats exposed to chronic hypoxia (17) and quantified as an early abnormality in the monocrotaline model (28), and this suggested increased elastolytic activity. We therefore chose a time when hypertrophy was evident, i.e., 10 days of exposure, to count the number of breaks in the elastic lamina and the number of myoendothelial junctions in small muscular arteries, but it is possible that the repair mechanism may have been complete.

Since the increased vascular elastolytic activity measured was inhibited by SC-39026, we have at least supportive evidence that this enzyme may play a contributing role in the pathogenesis of the hypoxia-induced pulmonary arterial changes. We cannot, for certain, rule out the possibility that some other mechanism is involved and the elastase inhibitor we used has other unrelated properties. Our most recent studies in monocrotaline-injected rats would, however, indicate that increased central pulmonary artery elastolytic activity not only precedes vascular changes but is predictive of progression versus regression (33). The lack of inhibition of medial hypertrophy in SC-39026-treated hypoxic rats, despite the reduced elastolytic activity in large arteries, requires explanation. It is possible that the increased elastolytic activity in the central pulmonary arteries of hypoxic rats is not directly related to the subsequent development of medial hypertrophy or alternatively, since the compound was administered orally, a continuous level of inhibition was not maintained. We favor the latter explanation, since monocrotaline-injected rats given SC-39026 (6) developed medial hypertrophy, whereas those given the analogue SC-37698 intravenously were protected (33), as were the hypoxic rats in this study that were administered A_1-PI by continuous infusion.

The source of the elastolytic activity is unknown. Elastases are found in neutrophils (1), platelets (10), macrophages (30), smooth muscle cells (5), and endothelial cells (31). Smooth muscle cells produce a serine elastase, which may induce elastin degradation in systemic arteries in association with atherosclerosis (22). Neutrophils have not been found adherent to or inside the artery wall of chronically hypoxic rats either in this study or in the work of others (16, 17). Increased endothelial elastase has also been suggested by immunocytochemical studies in rats with spontaneous hypertension (31). Hypoxic injury to alveolar macrophages might cause the release of an elastase (1), but this would not explain why alveolar structural changes are absent. We tried to detect elastolytic activity in the small pulmonary arteries using a human neutrophil elastase antibody with immunofluorescence and immunogold electron microscopy. The human neutrophil elastase antibody did not cross-react with the elastase in rat pulmonary artery wall. The purification of an elastase from rat pulmonary artery and the production of a specific antibody will allow more direct investigation of the role of elastolytic activity in hypoxia-induced muscularization of peripheral arteries.

We appreciate the help of Mike Ho, Lily Morikawa, and Julia Hwang for preparing the histology slides and Joan Jowlabar, Rebbie Pamintuan, and Evangeline Moodalie for secretarial assistance. We thank, Dr. Geraldine Kent, Director of the Animal Facility of the Research Institute, Helen Mcleod of Surgical Research, and Mike Starr and Eva Struthers of Visual Education. K. Maruyama also expresses personal thanks and appreciation to Dr. Robert E. Creighton, Director of Anesthesia at the Hospital for Sick Children, and especially to Dr. Frederick A. Burrows, Senior Staff Anesthetist for continuous support, encouragement, and guidance.

This study was supported by Grant T-724 from The Heart and Stroke Foundation of Ontario and by the Searle Research Foundation. K. Maruyama was a fellow of the Medical Research Council of Canada and is currently in the Department of Anesthesiology at Mie University Hospital, 2-174 Edobashi, Tsu, Mie 514, Japan. C. Ye was in part supported by a scholarship from the People's Republic of China. M. Woo received a John D. Schultz Summer Studentship from the Heart and Stroke Foundation of Ontario, and H. Venkatacharya was awarded a Summer Studentship from the Cystic Fibrosis Foundation of Canada. M. Rabinovitch is a Career Investigator of the Heart and Stroke Foundation of Ontario.

Address for reprint requests: M. Rabinovitch, Cardiovascular Research, The Hospital for Sick Children, 555 University Ave., Toronto, Ontario M5G 1X8, Canada.

Received 20 August 1990; accepted in final form 23 July 1991.

REFERENCES

1. CAMPBELL, E. J., AND M. S. WALD. Hypoxic injury to human alveolar macrophages accelerates release of previously bound neu-

trophil elastase. *Am. Rev. Respir. Dis.* 127: 631–635, 1983.
2. FOURNEL, M. A., J. O. NEWGREN, C. M. BETANCOURT, AND R. G. IRWIN. Preclinical evaluation of α-1-proteinase inhibitor. *Am. J. Med.* 84 *Suppl.*: 43S–47S, 1988.
3. GOLDSTEIN, R. A., AND B. C. STARCHER. Urinary excretion of elastin peptides containing desmosine after intratracheal injection of elastase in hamsters. *J. Clin. Invest.* 61: 1286–1290, 1978.
4. HYDE, L. W., W. D. BLACKBURN, M. H. IRWIN, AND D. R. ABRAHAMSON. Degradation of basement membrane laminin by human neutrophil elastase and cathepsin G (Abstract). *Am. J. Pathol.* 136: 1267, 1990.
5. HORNEBECK, W., D. BRECHEMIER, M. C. BOURDILLON, AND L. ROBERT. Isolation and partial characterization of an elastase-like protease from rat aorta smooth muscle cells. Possible role in the regulation of elastin biosynthesis. *Conn. Tiss. Res.* 8: 245–249, 1981.
6. ILKIW, R., L. TODOROVICH-HUNTER, K. MARUYAMA, J. SHIN, AND M. RABINOVITCH. SC-39026, a serine elastase inhibitor, prevents muscularization of peripheral arteries, suggesting a mechanism of monocrotaline-induced pulmonary hypertension in rats. *Circ. Res.* 64: 814–825, 1989.
7. KERR, J. S., C. L. RUPPERT, C. A. TOZZI, J. A. NEUBAUER, H. M. FRANKEL, S. Y. YU, AND D. J. RILEY. Reduction of chronic hypoxic pulmonary hypertension in the rat by an inhibitor of collagen production. *Am. Rev. Respir. Dis.* 135: 300–306, 1987.
8. LABOURENE, J. I., J. G. COLES, D. J. JOHNSON, A. MEHRA, F. W. KEELEY, AND M. RABINOVITCH. Alterations in elastin and collagen related to the mechanism of progressive pulmonary venous obstruction in a piglet model: a hemodynamic, ultrastructural and biochemical study. *Circ. Res.* 66: 438–456, 1989.
9. LEAKE, D. S., W. HORNEBECK, D. BRECHEMIER, L. ROBERT, AND T. J. PETERS. Properties and subcellular localization of elastase-like activities of arterial smooth muscle cells in culture. *Biochim. Biophys. Acta* 761: 41–47, 1983.
10. LEGRAND, Y., G. PIGNAUD, J. P. CAEN, B. ROBERT, AND L. ROBERT. Separation of human blood platelet elastase and proelastase by affinity chromatography. *Biochem. Biophys. Res. Commun.* 63: 224–231, 1975.
11. LOW, R. B., W. S. STIREWALT, P. HULTGREN, E. F. LOW, AND B. C. STARCHER. Changes in collagen and elastin in rabbit right ventricular pressure overload. *Biochem. J.* 263: 709–713, 1989.
12. MAINARDI, C. L., S. N. DIXIT, AND A. H. KANG. Degradation of type IV collagen (Basement Membrane) by a proteinase isolated from human polymorphonuclear leukocyte granules. *J. Biol. Chem.* 255: 5435–5441, 1980.
13. MCDONALD, J. A., AND D. G. KELLEY. Degradation of fibronectin by human leukocyte elastase. *J. Biol. Chem.* 255: 8848–8858, 1980.
14. MECHAM, R. P., J. G. MADARAS, AND R. M. SENIOR. Extracellular matrix-specific induction of elastogenic differentiation and maintenance of phenotypic stability in bovine ligament fibroblasts. *J. Cell. Biol.* 98: 1804–1812, 1984.
15. MECHAM, R. P., L. A. WHITEHOUSE, D. S. WRENN, W. C. PARKS, G. L. GRIFFIN, R. M. SENIOR, E. C. CROUCH, K. R. STENMARK, AND N. F. VOELKEL. Smooth muscle-mediated connective tissue remodeling in pulmonary hypertension. *Science Wash. DC* 237: 423–426, 1987.
16. MEYRICK, B., AND L. REID. Endothelial and subintimal changes in rat hilar pulmonary artery during recovery from hypoxia. *Lab. Invest.* 42: 603–615, 1980.
17. MEYRICK, B., AND L. REID. The effect of continued hypoxia on rat pulmonary arterial circulation. *Lab. Invest.* 38: 188–200, 1978.
18. NAKAO, A., R. A. PARTIS, G. P. JUNG, AND R. A. MUELLER. SC-39026, a specific human neutrophil elastase inhibitor. *Biochem. Biophys. Res. Commun.* 147: 666–674, 1987.
19. RABINOVITCH, M., W. J. GAMBLE, A. S. NADAS, O. S. MIETTINEN, AND L. REID. Rat pulmonary circulation after chronic hypoxia: hemodynamic and structural features. *Am. J. Physiol.* 236 (*Heart Circ. Physiol.* 5): H818–H827, 1979.
20. RABINOVITCH, M., M. A. KONSTAM, W. J. GAMBLE, N. PAPANICOLAOU, M. J. ARONOVITZ, S. TREVES, AND L. REID. Changes in pulmonary blood flow affect vascular response to chronic hypoxia in rats. *Circ. Res.* 52: 432–441, 1983.
21. RABINOVITCH, M., M. MULLEN, H. C. ROSENBERG, K. MARUYAMA, H. O'BRODOVICH, AND P. M. OLLEY. Angiotensin II prevents hypoxic pulmonary hypertension and vascular changes in rat. *Am. J. Physiol.* 245 (*Heart Circ. Physiol.* 14): H500–H508, 1988.
22. ROBERT, L., AND A. M. ROBERT. Elastin, elastase and arteriosclerosis. In: *Frontiers of Matrix Biology*, edited by A. M. Robert and L. Robert. Basel, Switzerland: Karger, 1980, vol. 8, p. 130–173.
23. ROSENBERG, H. C., AND M. RABINOVITCH. Endothelial injury and vascular reactivity in monocrotaline pulmonary hypertension. *Am. J. Physiol.* 255 (*Heart Circ. Physiol.* 24): H1484–H1491, 1988.
24. ROUGHLEY, P. J., AND A. J. BARRETT. The degradation of cartilage proteoglycans by tissue proteinases. *Biochem. J.* 167: 629–637, 1977.
25. SANDISON, J. C. Observations in the growth of blood vessels as seen in the transparent chamber introduced into the rabbit's ear. *Am. J. Anat.* 41: 475–496, 1928.
26. SILVER, M. M., AND S. A. HEARN. Postembedding immunoelectron microscopy using protein A-gold. *Ultrastruct. Pathol.* 11: 693–703, 1987.
27. STONE, P. J., S. M. MORRIS, B. M. MARTIN, M. P. MCMAHON, B. FARIS, AND C. FRANZBLAU. Repair of protease-damaged elastin in neonatal rat aortic smooth muscle cell cultures. *J. Clin. Invest.* 82: 1644–1654, 1988.
29. TODOROVICH-HUNTER, L., D. J. JOHNSON, P. RANGER, F. W. KEELEY, AND M. RABINOVITCH. Altered elastin and collagen synthesis associated with progressive pulmonary hypertension induced by monocrotaline. A biochemical and ultrastructural study. *Lab. Invest.* 58: 184–195, 1988.
30. WERB, Z., M. J. BANDA, AND P. A. JONES. Degradation of connective tissue matrices by macrophages. *J. Exp. Med.* 152: 1340–1357, 1980.
31. YAMADA, E., F. HAZAMA, H. KATAOKA, S. AMANO, M. SASAHARA, K. KAYEMBE, AND K. KATAYAMA. Elastase-like enzyme in the aorta of spontaneously hypertensive rats. *Virchows Arch. Cell. Pathol.* 44: 241–245, 1983.
32. YASUTAKE, A., AND J. C. POWERS. Reactivity of human leukocyte elastase and porcine pancreatic elastase toward peptide 4-nitroanilides containing model desmosine residues. Evidence that human leukocyte elastase is selective for cross-linked regions of elastin. *Biochemistry* 20: 3675–3679, 1981.
33. YE, C., AND M. RABINOVITCH. Inhibition of elastolysis by SC-37698 reduces development and progression of monocrotaline pulmonary hypertension. *Am. J. Physiol.* 261 (*Heart Circ. Physiol.* 30): H1255–H1267, 1991.

NPL

STIC-ILL

From: Chen, Shin-Lin
Sent: Thursday, January 20, 2000 7:34 AM
To: STIC-ILL
Subject: articles

Please provide the following articles by 1-24-00. Thanks!
Serial No. 09/258,217.

1. Bizbiz et al., Atherosclerosis, 1997 (May), 131(1), p. 73-78.

2. Bolobnesi et al., Monaldi Archives for Chest Disease, 1994 (April), 49 (2), 144-149.

3. Maruyama et al., Am. J. Physiol., 1991, 261 (6, pt.2), H1716-H1726.

Ilkiw et al., Circulation Research, 1989 (April), 64 (4), p. 814-825.

Shin-Lin Chen
AU 1633
CM1 12E03
(703)305-1678

ELSEVIER

Atherosclerosis 131 (1997) 73–78

ATHEROSCLEROSIS

Aging of the vascular wall: serum concentration of elastin peptides and elastase inhibitors in relation to cardiovascular risk factors. The EVA study

L. Bizbiz [a,*], A. Alpérovitch [b], L. Robert [a], the EVA Group

[a] *Laboratoire de Biologie Cellulaire, Université Paris VII, tour 23/33, case 7128, 1er étage, 2, Place Jussieu, 75005 Paris, France*
[b] *U 330 INSERM, CHV Pitié - Salpêtriere, 47 Bld de l'Hopital, 75013 Paris, France*

Received 15 January 1996; received in revised form 12 December 1996; accepted 7 January 1997

Abstract

The relations of biological markers of extracellular matrix (plasma elastin peptides and elastase inhibitors) to the clinical history of cardiovascular diseases and risk factors for atherosclerosis were examined in a large population study (the EVA Study) on vascular and cognitive aging performed in 1389 men and women aged 59–71 years. A moderate decrease in elastin peptides was observed in women with a self-reported history of coronary heart disease ($P < 0.091$) and stroke ($P < 0.03$) as well as with diabetes ($P < 0.043$). Similar but non-significant trends were found in men. Furthermore, elastin peptides were significantly and positively correlated to HDL-cholesterol and apolipoprotein A1 in both sexes. On the other hand, elastase inhibitor titers were significantly higher in women than in men. A moderate increase was also found in men ($P < 0.097$) and women ($P < 0.068$) with a history of coronary heart disease that reached significance level after pooling both sexes ($P < 0.014$). Furthermore, elastase inhibitor titers were significantly and positively related to fibrinogen and C reactive protein in either sex. No consistent associations were observed between both biological markers of extracellular matrix and age, blood pressure, body mass index and tobacco or alcohol consumption. These results suggest that a decrease in elastin peptides and an increase in elastase inhibitors might be associated with risk factors of atherogenesis as well as with atherosclerosis-related diseases. © 1997 Elsevier Ireland Science Ltd.

Keywords: Aging; Arteriosclerosis; Elastin; Elastases; Elastin peptides; Elastase inhibitors; Epidemiology

1. Introduction

The purpose of this study was to investigate the possible significance of serial determinations of serum constituents related to the degradation of extracellular matrix components of the vascular wall during aging and the development of arteriosclerosis and their correlation to other atheroselerotic risk factors. It was shown by several investigators that vascular extracellular matrix and especially elastin fibers are degraded during aging and atherogenesis [1,2].

The loss of elasticity and increasing rigidity of the aging arterial wall can be attributed to loss of elastin fiber integrity and stiffening of the collagen fiber network by maintained or increased synthesis and crosslinking by the Maillard reaction [3]. The loss of vascular elasticity, the so called 'windkessel' effect, is considered as one of the factors leading progressively to severe arteriosclerosis and heart insufficiency in elderly patients [4,5]. Elastase type enzymes attacking elastic fibers, present on smooth muscle cells [6] endothelial cells [7] and also in the serum [8] can also attack other matrix components and especially fibronectin [9]. Among the parameters which might be related to this process and amenable to serial clinical determinations are the plasma concentration of elastin degradation products, elastin peptides, and serum elastase inhibitors. A previous study described similar investiga-

* Corresponding author.

PII S0021-9150(97)06076-0

tions with serum elastase titers [8] and correlations with lung emphysema and atherosclerosis have been reported [10–12]. We also proposed an ELISA-procedure for plasma elastin peptide determinations and a serial procedure for serum elastase inhibitor determinations [12,13]. In a previous study on 270 subjects elevated levels of elastin peptides were found in some hyperlipidemias and obstructive arteriopathies [12].

In the present study, we applied these procedures to the determination of elastin peptides, and elastase inhibitors in the sera of a larger population of elderly males and females as part of an epidemiological study on vascular and cognitive aging, the EVA Study [8,14]. We aimed to assess the cross sectional associations between these blood born parameters related to the extracellular matrix of the vessel wall and the clinical history of cardiovascular disease and risk factors.

2. Materials and methods

2.1. Study population

The EVA Study is a 4-year longitudinal study on cognitive and vascular aging [8,14]. The study population was composed of volunteers aged 59–71 years recruited from electoral rolls of the City of Nantes (Western France) and, to a lesser extent, via information campaigns. When a subject was recruited, his or her spouse was systematically asked to participate in the study if he or she was in the desirable age range. During the baseline visit which took place between June 1991 and July 1993, 1389 subjects were recruited. The study protocol was approved by the Comité d'éthique du Centre Hospitalier Universitaire de Kremlin-Bicêtre and written informed consent was obtained from all participants.

All participants were administered a standardized questionnaire which gave information about demographic background, occupation, medical history, drug use and personal habits such as cigarette and alcohol consumptions. With respect to smoking behavior, subjects were classified as current smokers, former smokers and non-smokers. Alcohol consumption was determined from the subject's estimate of the average amount of alcoholic beverages ingested weekly and expressed in ml/alcohol/day. Two independent measurements of systolic and diastolic blood pressure were made with a digital electronic tensiometer (SP9 Spengler) after a 10 min rest and the mean was used in the analysis. Body mass index was computed as weight divided by height squared (kg/m^2). Hypertension was defined as systolic blood pressure ≥ 160 mmHg or diastolic blood pressure ≥ 95 mmHg or use of antihypertensive drugs. A self-reported history of coronary heart disease (myocardial infarction or angina pectoris) and stroke was also recorded. A subject was considered diabetic if he/she reported a medical history of diabetes or use of antidiabetic drugs or had a fasting plasma glucose level ≥ 1.40 g/l.

2.2. Laboratory procedures

2.2.1. Standard biochemical parameters

Methods of determination of total cholesterol, HDL cholesterol, apolipoprotein A1 and B and triglycerides are described elsewhere [8,14].

2.2.2. Elastin peptides

Elastin peptides were determined by ELISA procedures as previously described [12] with some modifications [13]. The specificity of the monoclonal antibody used (A1, 2) are also described elsewhere [15].

2.2.3. Serum elastase inhibitor titers

The determination of elastase inhibitor titers is described in detail in [13]. Briefly, 10 μl of serum samples were pipetted in 5 ml polypropylene centrifuge tubes, 100 μl of pancreatic elastase is added (type IV Sigma, 20 U/ml) with 10 μl of an elastin fiber suspension (200 mg/ml) kept at constant agitation in order to assure a uniform distribution of the fibers during pipetting. The tubes were incubated for 2 h at 37°C with constant shaking then centrifuged at 5000 rpm for 10 min at 4°C and the radioactivity of the supenatent measured in a 1209 Rack β counter (Pharmacia). Inhibitory titers were calculated from the ratio of radioactivity released in the absence of serum to activities determined in the presence of serum. All determinations were carried out in duplicate and expressed as % inhibition.

Methods for determinations of the other blood parameters are described in [8,14].

2.3. Statistical analysis

Standard procedures from the Statistical Analysis System (SAS, Cary, NC) were used. Differences in mean values of elastin peptides and elastase inhibitor titers across categories were tested by ANOVA. Pearson's correlation coefficients were used to assess the associations between these biological parameters and quantitative variables. Triglycerides were log-transformed for statistical testing [8,14].

3. Results

As indicated in Fig. 1, there were no sex differences in the distribution or in the mean levels of elastin peptides (8.31 ± 4.43 versus 8.39 ± 4.40 μg/ml in men and women respectively). Mean values of elastin peptides according to the presence of a self-reported his-

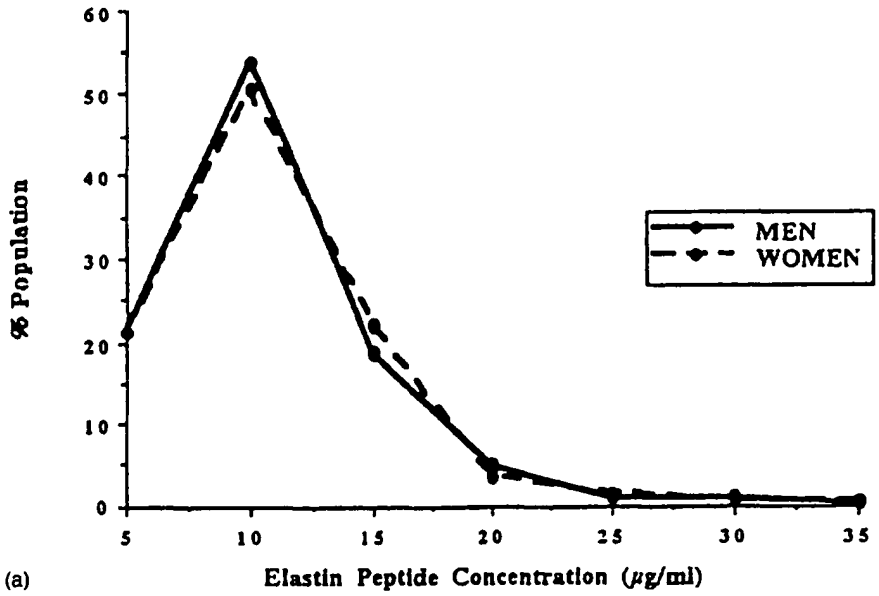

Fig. 1. Distribution of elastin peptide concentrations in the EVA population.

tory of coronary heart disease and stroke, of hypertension and diabetes are shown in Table 1. Significant or borderline negative associations were observed between the presence of coronary heart disease, stroke and diabetes and the levels of elastin peptides in women. In men, similar but non significant trends were found with a history of coronary heart disease and stroke. When both sexes were pooled, the association with stroke was significant (sex-adjusted mean ± S.E.M.: 8.40 ± 0.13 versus 6.50 ± 0.82 μg/ml, $P < 0.022$) but the association with coronary heart disease fell short of significance (sex-adjusted mean ± S.E.M.: 8.42 ± 0.13 versus 7.47 ± 0.50 μg/ml, $P < 0.064$). Elastin peptides were not significantly associated with age, body mass index, blood pressure or tobacco and alcohol consumption. Correlation coefficients with lipid parameters, fibrinogen and C reactive protein are presented in Table 2. In either sex, elastin peptides were positively and significantly related to HDL cholesterol and apolipoprotein A1, whereas they were negatively related to triglycerides and apolipoprotein B in men only.

As shown in Fig. 2, the distribution curve of elastin inhibitor titers was slightly shifted to lower values in men with mean values significantly lower in men than

Table 1
Mean values of plasma elastin peptides according to the clinical history of cardiovascular disease, hypertension and diabetes

	Men		Women	
	n	mean ± S.D.	*n*	mean ± S.D.
Coronary heart diseaes				
No	471	8.37 ± 4.49	690	8.45 ± 4.45
Yes	41	7.69 ± 3.66	38	7.21 ± 3.26
		NS		$P < 0.091$
Stroke				
No	499	8.35 ± 4.44	712	8.44 ± 4.41
Yes	13	7.03 ± 3.79	16	6.06 ± 3.24
		NS		$P < 0.03$
Hypertension				
No	316	8.51 ± 4.64	519	8.52 ± 4.41
Yes	196	8.00 ± 4.06	209	8.08 ± 4.38
		NS		NS
Diabetes				
No	466	8.32 ± 4.41	709	8.44 ± 4.43
Yes	46	8.24 ± 4.67	19	6.36 ± 2.69
		NS		$P < 0.043$

Table 2
Correlation coefficients between plasma elastin peptides, elastase inhibitors and biological risk factors for atherosclerosis

	Elastin peptides		Elastase inhibitors	
	Men	Women	Men	Women
Total cholesterol	−0.01	0.03	−0.10*	−0.03
HDL-cholesterol	0.23*	0.13	−0.04	0.02
LDL-cholesterol	−0.08	0.00	0.11*	−0.02
Apoprotein A1	0. 18**	0.08*	0.07	−0.05
Apoprotein B	−0.15**	− 0.04	0.06	0.08*
Triglycerides	−0.10*	−0.07	0.05	0.05
Fibrinogen	0.00	0.05	0.31**	0. 12**
C reactive protein	−0.06	0.00	0. 17**	0. 18**

* $P < 0.05$; ** $P < 0.001$; ** $P < 0.01$. Because of missing data, the number of subjects ranged from 497 to 529 in men and from 698 to 732 in women.

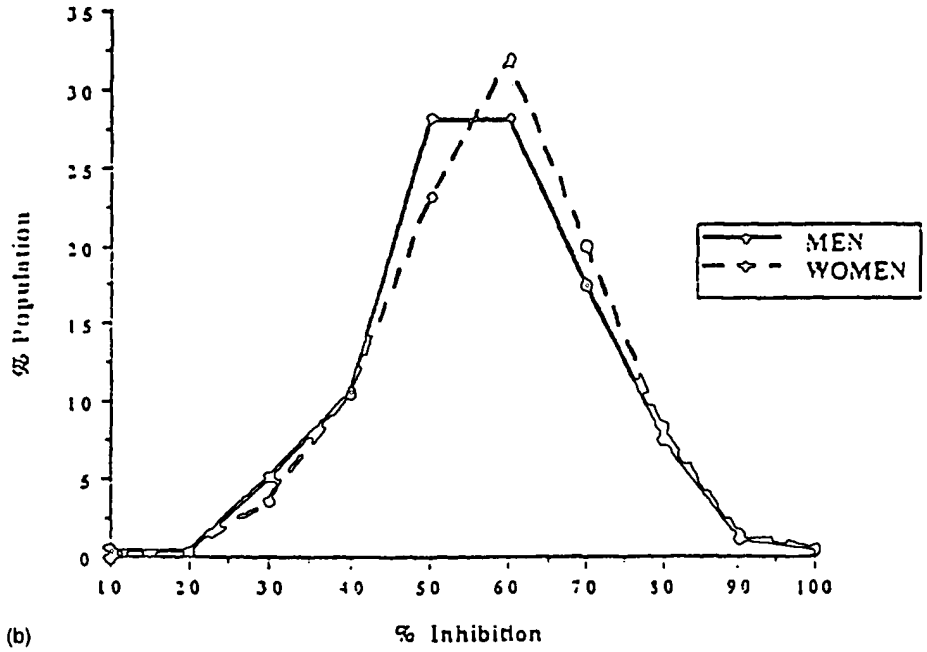

Fig. 2. Distribution of elastase inhibitor titer in the EVA population.

in women (mean ± S.D.: 51.9 ± 13.6 versus 53.8 ± 12.9%, $P < 0.02$). In either sex, elastin inhibitor titers tended to be higher in subjects with coronary heart disease than in those without (mean ± S.D.: 51.6 ± 13.5 versus 55.0 ± 14.3% in men, $P < 0.097$; 53.6 ± 13.0 versus 57.4 ± 10.3% in women, $P < 0.068$). In pooled men and women, this association was significant after adjustment for sex ($P < 0.014$). No significant associations were found with a history of stroke, diabetes and hypertension in either sex. Furthermore, elastase inhibitor titers were not related to age, blood pressure and tobacco or alcohol consumption. Only a weak positive correlation was observed with body mass index in women ($r = 0.082$, $P < 0.03$). Correlation coefficients with lipid parameters, fibrinogen and C reactive protein are also shown in Table 2. Fibrinogen and C reactive protein were the strongest correlates of elastase inhibitor titers in both men and women. Weak negative associations with total cholesterol and LDL cholesterol were observed only in men.

4. Discussion

The purpose of this study was to explore possible correlations between serum parameters related to elastin fiber degradation and other clinical or biological parameters of atherogenesis. A previous study [8] reported some significant correlations between serum elastase titers and clinical or biological parameters of atherogenesis and an increase in serum elastase activity with increasing alcohol consumption. The present study also revealed some significant correlations between elastin peptides and elastase inhibitor titers with several of the atherosclerotic risk factors and mainly with some of the related diseases: coronary heart disease, stroke and diabetes (Table 1). Elastin peptide concentrations were shown to be positively correlated to apolipoprotein A1 and HDL-cholesterol values. Serum elastase inhibitor titers are positively correlated to fibrinogen and negatively correlated to total cholesterol and LDL-cholesterol values, (Table 2) with the reservation concerning sexes. Some correlations are significant only for males or females and some are significant for both sexes.

The negative correlations between elastase inhibitor titers and lipidic parameters (Table 2) are too weak to be interpreted as a protective effect of higher elastase inhibitor titers. The positive correlation between elastase inhibitors and fibrinogen may be attributed to their correlated increase as acute phase reactants of hepatic origin. The main component of serum elastase inhibitors, α_1-protease inhibitor (α_1-Pi) is known to be an acute phase glycoprotein [16]. As shown previously by Jayle et al. [16] angina patients frequently exhibit increased acute phase glycoprotein values as for instance serum haptoglobine. α_1Pi, the principal component of the serum inhibiting serine-elastases, is one of the acute phase glycoproteins.

Elastin peptides showed a positive correlation with apolipoprotein A1 and HDL-cholesterol, parameters considered to have a protective value for cardiovascular disease [17]. Previous studies have shown that elastin peptides acting on the endothelial elastin receptor in-

duce an NO-dependent vasodilatation [18]. These results are in agreement with previous experiments on cholesterol feeding in rabbits, which showed a protective effect for elastin peptide treatment against the development of cholesterol induced atherosclerotic lesions [19].

The decrease in elastin peptides in female stroke and diabetic patients would be in agreement with the above interpretation. Further studies are necessary to elucidate the relationship between the serum level of elastin degradation products and specific cardiovascular diseases. These peptides may be derived from the degradation of elastic fibers but also from the post-synthetic degradation of newly synthesised tropoelastin [20]. The selective detection of these two types of degradation products might shed further light on this problem.

Serum elastase titers [8], serum elastase inhibitors and elastin peptides (in the present study) showed no significant correlation to each other, suggesting independent mechanisms for the regulation of these three elastin related serum parameters. Most serum elastase activity (80–90%) is due to metalloproteases, not inhibited by the major circulating elastase inhibitor, α_1Pi, which acts only on serine-proteases. The exact role of serum elastase activity in the degradation of vascular elastic fibers remains to be investigated. Elastase-type proteases produced by vascular smooth muscle cells [6] and endothelial cells [7] could also be involved. Although other tissues such as lung parenchyma and skin could contribute to elastin degradation products most of the elastin fibers of the organism are present in the vascular wall. Thoracic aorta contains 30–40% of elastin and abdominal aorta about 20% [21]. The degradation of vascular elastic fibers in atherogenesis has been previously demonstrated [22,23]. Recent results concerning the presence of a receptor reacting with elastin peptides on vascular cells and white blood cells [5,24–26] as well as the physiological functions attributable to this receptor [8,25,27] suggest an important physio–pathological role for circulating elastin peptides. The continuous exposure of the elastin receptor to saturating levels of elastin peptides might well represent a crucial mechanism in the age dependent modifications of the vascular wall [5].

Acknowledgements

Several laboratories and researchers contributed to the determinations used for the calculations of correlation between elastin peptides, elastase inhibitors and other parameters. We gratefully acknowledge the contributions of Professor Juhan-Vague (Laboratoire d'Hématologie, Hôpital la Timone, Marseille, France) for fibrinogen and PCR deteminations. This study was supported by a grant from MSD-INSERM and the Fondation Pierre Louis, Fondation de France.

References

[1] Bouissou H, Pieraggi MT, Julian M, Douste Blazy L. Cutaneous aging. Its relation with arteriosclerosis and atheroma. Front Matrix Biol 1973;1:190–211.
[2] Robert L, Robert AM. Elastin, elastase and atherosclerosis. Front Matrix Biol 1980;8:130–173.
[3] Cox CS. Roles of Maillard Reactions in Diseases. London: HMSO, 1991.
[4] Burger M. Alterm und Krankheit. Leipzig: Georg Thieme, 1947.
[5] Robert L. Aging of vascular wall and atherogenesis, role of the elastin-laminin receptor. Atherosclerosis 1996;123:169–179.
[6] Hornebeck W, Brechemier D, Soleilhac JM, Bourdillon MC, Robert L. Studies on rat aorta smooth muscle cells elastase activity. In: Reddi AH (ed). Extracellular Matrix: Structure and Function. New York: Alan R. Liss, 1985;25:269–282.
[7] Menasche M, Hornebeck W, Robert L, Legrand Y. Elastase-like activity in cultured aortic endothelial cells. Thromb Res 1989;53:11–18.
[8] Bizbiz L, Bonithon-Kopp C, Ducimetière P et al. Relation of serum elastase activity to ultrasonographically assessed carotid artery wall lesions and cardiovascular risk factors. The EVA study. Atherosclerosis 1996;120:47–55.
[9] Labat-Robert J. Apport des enzymes protéolytiques à la connaissance des fonctions biologiques de la fibronectine. Pathol Biol 1990;38:1005–1009.
[10] Darnule TV, McKee M, Darnule AT, Turino GM, Mandl I. Solid-phase radioimmuno-assay for estimation of elastin peptides in human sera. Anal Biochem 1982;122:302.
[11] Kucich U, Christner P, Lippmann M et al. Immunologic measurement of elastin-derived peptides in human serum. Am Rev Respir Dis 1983;127:S28.
[12] Fülöp T, Wei SM, Robert L, Jacob MP. Determination of elastin peptides in normal and arteriosclerotic human sera by ELISA. Clin Physiol Biochem 1990;8:273–282.
[13] Bizbiz L, Robert L. Micro-methods for serial determinations of elastin metabolism parameters in blood plasma and serum. Pathol Biol 1996;44:694–700.
[14] Bonithon-Kopp C, Touboul PJ, Berr C et al. Relation of intima-media thickness to atherosclerotic plaques in the carotid arteries—the EVA Study. Arterioscler Thromb Vasc Biol 1996;16:310–316.
[15] Wei SM, Erdei J, Fülöp T, Robert L, Jacob MP. Elastin peptide concentration in human serum: variation with antibodies and elastin peptides used for the enzyme-linked immunosorbent assay. J Immun Methods 1993;164:175–187.
[16] Jayle MF, Coumel H, Farges JP, Baylon H, Dulac JF, Dormann E. Les modifications de la formule protéique du sérum dans l'infarctus du myocarde. Arch Mal Coeur Vaisseaux. 1952;4:328.
[17] Jacotot B. Epidémiologie et facteurs de risque In: Jacotot B (ed). Paris: Athérosclérose, Sandoz, 1994;2746.
[18] Faury G, Ristori MT, Verdetti J, Jacob MP, Robert L. Effect of elastin peptides on vascular tone. J Vasc Res, 1995;32:112–119.
[19] Robert L, Jacob MP, Szemenyei K, Robert AM. Pharmacological properties of elastin peptides, their action on serum and aorta lipids and on the atherosclerotic process, in: Carlson LA and Olsson AG (eds). Treatment of hyperlipoproteinemia. New York: Raven Press 1984;185–188.
[20] Fülöp T, Jacob MP, Robert L. Biological effects of elastin peptides. In: Robert L and Hornebeck W (eds). Elastin and Elastases, I. Boca Raton, FL: CRC Press, 1989;201–210.
[21] Robert L, Hornebeck W. Elastin and Elastases, I, II. Boca Raton, FL: CRC Press, 1989.
[22] Balo J. Connective tissue changes in atherosclerosis. In: Hall DA (ed). International Review of Connective Tissue Research. New York: Academic Press, 1963;1:241–306.

[23] Bouissou H, Pieraggi Mth, Julian M. Aging of elastic tissue on skin and arteries. In: Robert L, Murata K and Nagai Y (eds). Degenerative Diseases of Connective Tissue and Aging. Tokyo: Kodansha, 1985;203–216.

[24] Hornebeck W, Tixier JM, Robert L. Inducible adhesion of mesenchymal cells to elastic fibers: elastonectin. Proc Natl Acad Sci USA 1986;83:5517–5520.

[25] Robert L, Jacob MP, Fülöp T, Timar J, Hornebeck W. Elastonectin and the elastin receptor. Pathol Biol 1989;37:736–741.

[26] Robert L. Interaction between cells and elastic fibers the elastin receptor and elastonectin. Connect Tissue 1993;25:219–225.

[27] Robert L, Jacob MP, Fülöp T. Elastin in blood vessels. In: The Molecular Biology and Pathology of Elastic Tissues. Ciba Symposium. ed. L. Robert, D.J. Chadwick, Chichester: Wiley, 1995;286–303.

STIC-ILL

279/93

From: Chen, Shin-Lin
Sent: Thursday, January 20, 2000 7:34 AM
To: STIC-ILL
Subject: articles

Please provide the following articles by 1-24-00. Thanks!
Serial No. 09/258,217.

1. Bizbiz et al., Atherosclerosis, 1997 (May), 131(1), p. 73-78.

2. Bolobnesi et al., Monaldi Archives for Chest Disease, 1994 (April), 49 (2), 144-149.

3. Maruyama et al., Am. J. Physiol., 1991, 261 (6, pt.2), H1716-H1726.

Ilkiw et al., Circulation Research, 1989 (April), 64 (4), p. 814-825.

Shin-Lin Chen
AU 1633
CM1 12E03
(703)305-1678

ZGE-00012069II

Monaldi Arch Chest Dis
1994; 49: 2, 144–149

Molecular bases for human leucocyte elastase inhibition

M. Bolognesi*+, K. Djinović-Carugo*, P. Ascenzi**

*Dipartimento di Genetica e Microbiologia, Università di Pavia, Pavia, Italy. +Centro Biotecnologie Avanzate, IST e Dipartimento di Fisica, Università di Genova, Genova, Italy. **Dipartimento di Scienza e Tecnologia del Farmaco, Università di Torino, Torino, Italy.

Correspondence: M. Bolognesi, Dipartimento di Genetica e Microbiologia, Università di Pavia, Via Abbiategrasso, 207.27100 Pavia, Italy.

Keywords: Human leukocyte elastase; inhibition mechanism; molecular bases.

ABSTRACT

Molecular bases for human leucocyte elastase inhibition. M. Bolognesi, K. Djinović-Carugo, P. Ascenzi.

Human leucocyte elastase is a serine proteinase involved in phagocytosis, defence against invading micro-organisms, degradation of elastin, collagen, proteoglycans, fibrinogen and fibrin, being also responsible for the digestion of damaged tissues and of the bacterial degradation products. Lack of the enzyme regulation is at the basis of pathological states, such as pulmonary emphysema, cystic fibrosis, rheumatoid arthritis, atherosclerosis and glomerulonephritis.

A detailed characterisation of the enzyme:inhibitor recognition process, based on extensive thermodynamic, kinetic and structural information, as well as on the comparative analysis with the homologous proteinase from porcine pancreas, is reported in the present review.

Monaldi Arch Chest Dis., 1994; 49: 2, 144–149.

Proteases and their zymogens play a central role in several biological processes, ranging from digestion to key regulatory mechanisms, such as coagulation and hormone release, and are also recognised in many diseases [1–6]. Therefore, the possibility of selectively influencing proteolytic activities by specific (natural or synthetic) inhibitors appears to be of considerable interest, in view of their potential therapeutic value as drugs [2, 4–6].

Among serine proteinases, human leucocyte elastase (HLE) is essential for phagocytosis and for defence against invading micro-organisms. Moreover, HLE is naturally involved in the degradation of elastin, collagen, proteoglycans, fibrinogen and fibrin, being also responsible for the digestion of damaged tissues and of the bacterial degradation products [4–8]. Lack of HLE regulation, generally due to an impaired balance between the enzyme and its natural inhibitors (α_1-proteinase inhibitor (α_1-PI), α_2-macroglobulin (α_2-M), and mucus proteinase inhibitor (MPI)), is at the basis of pathological states, such as pulmonary emphysema, cystic fibrosis, rheumatoid arthritis, atherosclerosis and glomerulonephritis.

Free radicals present in cigarette smoke have been shown to inactivate α_1-PI *in vitro* (the reactive site P_1 Met358 residue being oxidised to methionine sulphoxide), and are believed to cause deficiency of the active serine proteinase inhibitor in smokers' lungs. Thus, a decrease of native inhibitor concentration in the lung is thought to be a primary factor in the pathogenesis of pulmonary emphysema, associated with cigarette smoking. The decifiency of α_1-PI, however, is transient, and reversible on cessation of cigarette smoking [4–6]. Moreover, some individuals are genetically deficient in α_1-PI, the inhibitor being poorly secreted from the liver cells. This genetic defect has been related to the development of familial emphysema [4–6].

The proteolytic action of HLE can also be modulated by nonphysiological, but naturally occurring, protein serine proteinase inhibitors of the potato inhibitor type I family, *e.g.*, eglin c (the serine proteinase inhibitor from the leech *Hirudo medicinalis*), and of the Kunitz and Kazal families, *e.g.* the basic pancreatic trypsin inhibitor, the pancreatic secretory trypsin inhibitor and ovomucoid inhibitors. Moreover, low molecular weight synthetic compounds, such as peptide chloromethylketones, fluoroketones, peptide boronic or isocoumarinic compounds, as well as molecules based on the carbonylthiophene acylating substructure have been successfully tested as HLE inhibitors [1–6, 9–13].

X-ray crystallography has provided a comprehensive approach to the study of the catalytic and inhibition mechanisms in serine proteinases [14]. Analysis of the three-dimensional structure of free and complexed enzymes has unravelled the molecular organisation (at atomic resolution) of more than 30 protein structures belonging to the serine proteinase trypsin-chymotrypsin-elastase homology family (known as "chymotrypsin superfamily"). Thus, a reliable database has been established [14, 15], suitable for structure-function inhibition investigations, for simulations based on molecular mechanics and dynamics, as well as for homology modelling studies [16].

Molecular investigations have shown that HLE displays a structural organisation strongly reminiscent of homologous serine proteinases (such as porcine pancreatic elastase, or bovine α-chymotrypsin), with the conserved catalytic triad, based on residues His57, Asp102 and Ser195, located in a central cleft defined by the enzyme tertiary structure. Moreover, the fine details of the enzyme structure and, most notably, of the active site geometry and of substrate specificity subsites, have been analysed in the presence of different classes of inhibitors [14, 17–19].

The present review concerns aspects of HLE inhibition which are related to the rational study of enzyme:inhibitor recognition processes, and thus, potentially, to the design of new active therapeutic agents.

The inhibition mechanism of HLE

The minimum mechanism of HLE inhibition by (macro)molecular inhibitors [6, 20, 21] is given by:

$$E + I \underset{k_{off}}{\overset{k_{on}}{\rightleftarrows}} EI \xrightarrow{k_{+2}} EI^* \xrightarrow{k_{off}^*} E + I^* \quad (1)$$

where E is the enzyme, I and I* are the virgin and the modified (P_1-P_1' reactive site peptide bond hydrolysed) [22] inhibitor, respectively; EI and EI* are the stable adducts of the proteinase with the virgin or the modified inhibitor, k_{on} is the second order rate constant for the formation of the EI complex; k_{+2} is the first order rate constant for formation of the EI* adduct, k_{off} and k_{off}^* are the first order dissociation rate constant for the destabilisation of the EI and EI* complexes, respectively, and K_i ($=k_{on}/k_{off}$) is the equilibrium constant for the formation of the EI adduct. The HLE inhibition mechanism given in scheme 1 is reminiscent of the minimum three step catalytic mechanism of serine proteinases. Therefore, the main difference between an inhibitor and a substrate for the target proteinase is represented by the very different rates for the dissociation of the EI and EI* complexes. Indeed, a given inhibitor might be considered as a modified substrate which dissociates slowly [4–6, 20, 21].

From the pharmaceutical viewpoint, the potency of a serine proteinase inhibitor depends both on thermodynamic and kinetic parameters for the enzyme: inhibitor complex (de)stabilisation. Thus: 1) the affinity (for the target enzyme) must be very high ($K_i > 10^8$ M^{-1}); 2) the second order rate constant for complex formation must be fast ($k_{on} > 10^4$ M^{-1} s^{-1}); and 3) the first order rate for the dissociation of the binary complexes should be very slow (k_{off} and k_{off}^* $< 1\times10^{-4}$ s^{-1}). Accordingly, the therapeutic dose of the inhibitor should be low and the pharmaceutical effect should be fast and long-lasting.

Three-dimensional structure of HLE in relation to inhibitor binding

Owing to the strong conservation of primary structure in the chymotrypsin superfamily [16], HLE displays a tertiary structure which is strongly reminiscent of those observed for related serine proteinases (such as pancreatic elastase or α-chymotrypsin). The 218 amino acid polypeptide chain is organised in two domains, mostly built up by antiparallel β-barrel structure [17]; an α-helical segment is present in the C-terminal region of the molecule (fig. 1). The crevice defined by the two globular domains is the substrate (inhibitor) binding site, and hosts the conserved catalytic triad (His57, Asp102 and Ser195) responsible for the enzymatic cleavage of the substrate. In this structural/topological organisation, HLE is very similar to porcine pancreatic elastase, for which several crystallographic investigations are available, and the amino acid sequence of which shares 40% residue identities with HLE [23]. Some surface polypeptide loops of HLE, however, display unique geometry or limited conformational disorder in the crystal structures [17, 18].

As mentioned above, HLE activity is affected not only by its natural inhibitors (α_1-PI, α_2-M and MPI), but also by other protein serine proteinase inhibitors, the thermodynamic and kinetic parameters for binding of protein proteinase inhibitors to HLE spanning about seven orders of magnitude [5].

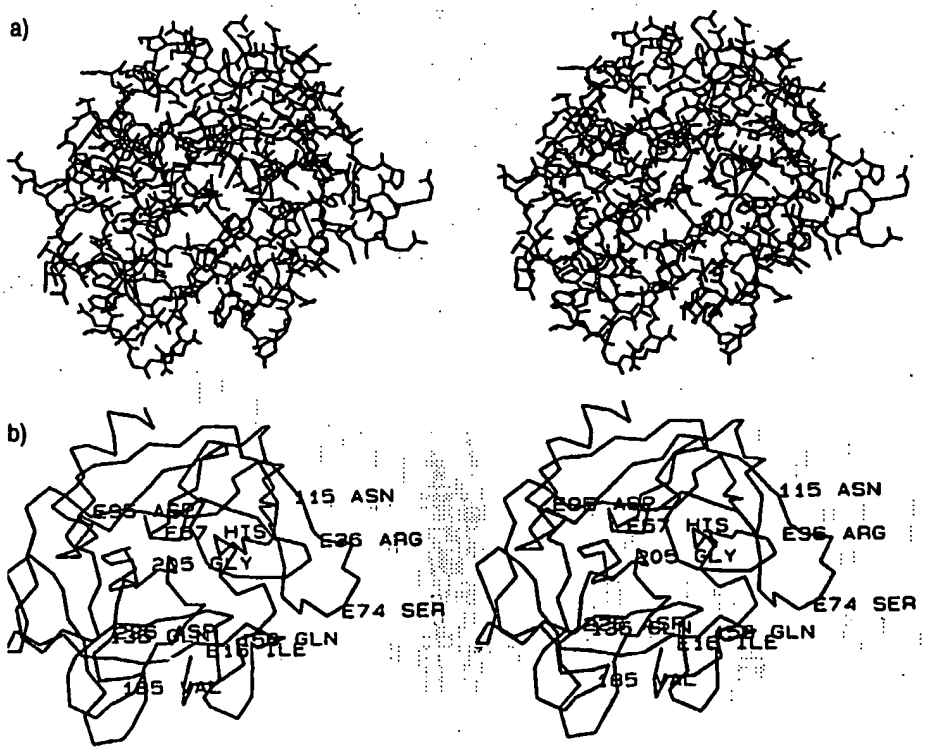

Fig. 1. – a) Stereo view of human leucocytes elastase (HLE) [17]. All amino acid residues have been included. b) Cα backbone of HLE [17]. The enzyme is drawn in the same orientation as given in (a). The active site crevice is visible in the central part of the molecule.

Crystallographic studies on inhibited HLE have provided reference structures which indicate the likely recognition and binding mode of an extended substrate (inhibitor) to the enzyme active site. Of particular interest is the complex of HLE with the third domain of the natural polypeptide inhibitor turkey ovomucoid (OMTKY3) [17]. As can be appreciated from inspection of figure 2, the globular protein inhibitor binds to the proteinase active site cleft through an extended loop of polypeptide structure. One specific inhibitor residue, the so-called "reactive-site" residue (P_1), is positioned in HLE primary specificity subsite (S_1), and properly positions the scissile peptide bond with respect to the catalytic triad residues. Proteinase:inhibitor recognition is extended to seven subsites from P_5 to P_3'. These interactions include specific hydrogen bonds to HLE polypeptide backbone atoms (involving residues Phe41, Ser214, Val216 and Gly218), as well as extended van der Waals and hydrophobic contacts between the inhibitor P_5–P_3' residues and the enzyme central region [17, 18]. Undoubtedly, however, a primary recognition event, as in other homologous serine proteinases, occurs at the S_1 specificity subsite, where a medium size hydrophobic pocket present in the HLE active centre hosts the P_1 residue of the inhibitor. This residue (Leu 18 in OMTKY3) in an ideal HLE substrate or inhibitor is expected to be an alkyl side-chain, such as Val.

Modulation of serine proteinase action by protein inhibitors (which could be potential substrates) is achieved through a series of subtle concurring factors, which stabilise the E:I complex, and prevent (or slowdown) hydrolysis of the reactive site bond. These factors are related mainly to the structural properties of the interacting partners, and include surface complementarity, restricted mobility of the (re)active site interacting loops and (re)active site limited accessibility to water molecules, as evidenced in several crystallographic studies on serine proteinase:protein inhibitor complexes [14, 24, 25].

Several inhibitors of HLE (*i.e.* peptide chloromethylketones and fluoroketones, saccharine derivatives, heterocyclic compounds, azapeptides, isocoumarins and the microbial inhibitor elastatinal) have proved to be effective in modulating the proteinase-induced development of emphysema in hamsters and mice. The inhibitors were found to be active when given intratracheally, orally, intraperitoneally or intravenously (coupled to albumin microspheres). It must be noted, however, that these compounds were active only when given one hour or less before the insult; at various times after the insult the inhibitors were generally found to be ineffective [2].

Among inhibitors acting as acylating agents of the catalytic residue Ser195, 2-[3-thiophenecarboxythio]-N-[dihydro-2(3H)-thiophenone-3-il]-propionamide (MR889) and 3-[2-thiophenecarboxythio]-propanoyl-4-thiazolidinecarboxylic acid (YS3025) inhibit not only the HLE catalysed hydrolysis of low molecular weight synthetic substrates, but also the *in vitro* cleavage of insoluble elastin, *i.e.* the physiological target of this serine proteinase [6, 11]. Furthermore, MR889 has been tested *in vivo* for potential toxicity, without observing any mortality after oral administration of up to 5 $g \cdot kg^{-1}$ body weight, in mice [11]. These findings are prerequisites for the therapeutic application of the two low molecular weight serine proteinase inhibitors MR889 and YS3025 [6, 11].

Concerning the inhibition mechanism of HLE by MR889 and YS3025, POWERS and BENGALI [4], RIZZI *et al.* [12] and DJINOVIĆ-CARUGO *et al.* [13] have shown that the serine proteinase:inhibitor adducts contain the thiophenecarbonyl moiety of the inhibitor covalently bound to the active site Ser195OG atom. Inspection of the X-ray three-dimensional structure of YS3025-inhibited porcine pancreatic elastase (figs. 3a and b) shows that the reactive site residue Ser195 is acylated by the inhibitor molecule, which reacts with the enzyme through hydrolysis of the thioester bond adjacent to the thiophene ring. The nucleophilic attack of Ser195OG atom on the inhibitor scissile bond is facilitated by proper location of the

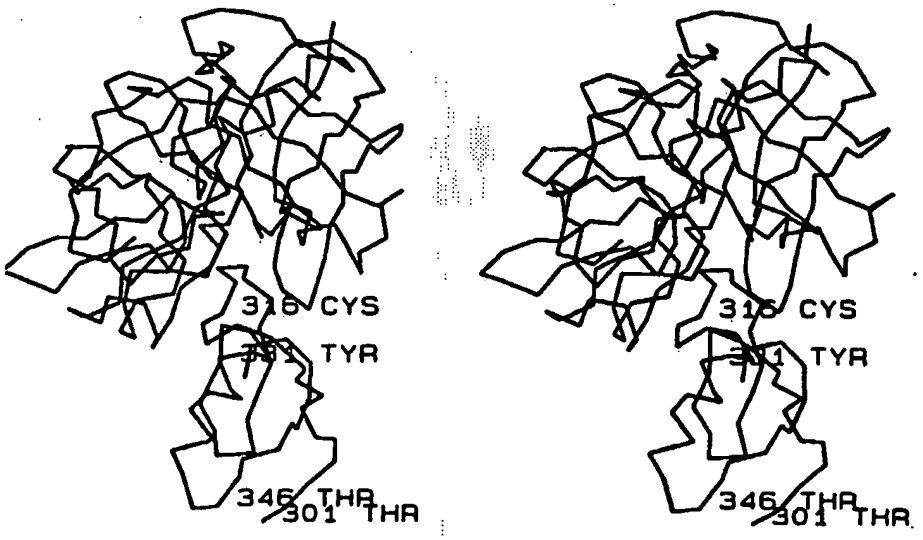

Fig. 2. – Cα skeleton representation of the human leucocyte elastase (HLE): Kazal inhibitor complex built on the basis of computer methods and stereochemical rules known for enzyme:inhibitor recognition. The inhibitor molecule is clearly depicted in the lower part of the figure, with residue numbering starting at 301. The active site crevice of HLE is particularly evident in this orientation.

YS3025 apolar thiophene ring in the porcine pancreatic elastase S_1 specificity pocket. The acyl-enzyme complex is stable for long periods (as compared to a conventional substrate), mostly because of an unfavourable orientation of the electrophile carbonyl carbon (involved in the acyl bond) of the proteinase active site, such that a deacylating (nucleophile) water molecule has impaired accessibility to it. Inspection of the crystal structures of acyl-enzyme complexes formed by YS3025 with homologous serine proteinases [13], shows that the general properties and features of the inhibition mechanism are valid throughout the entire chymotrypsin superfamily. Thus, rational modification of this class of inhibitors can be achieved in order to target the newly designed molecules toward serine proteinases endowed with different specificities (and acting in different metabolic compartments).

The inhibition mechanism of HLE by the active site directed tetrapeptides methoxysuccinyl-Ala-Ala-Pro-Ala(Val) chloromethylketones has also been elucidated by X-ray crystallography [18, 26]. The tetrapeptide inhibitors bind irreversibly to the active site of HLE. Covalent bond formation between the inhibitor Ala(Val) P_1 residue carbonyl carbon and HLE His57NE2 and Ser195OG atoms is observed;

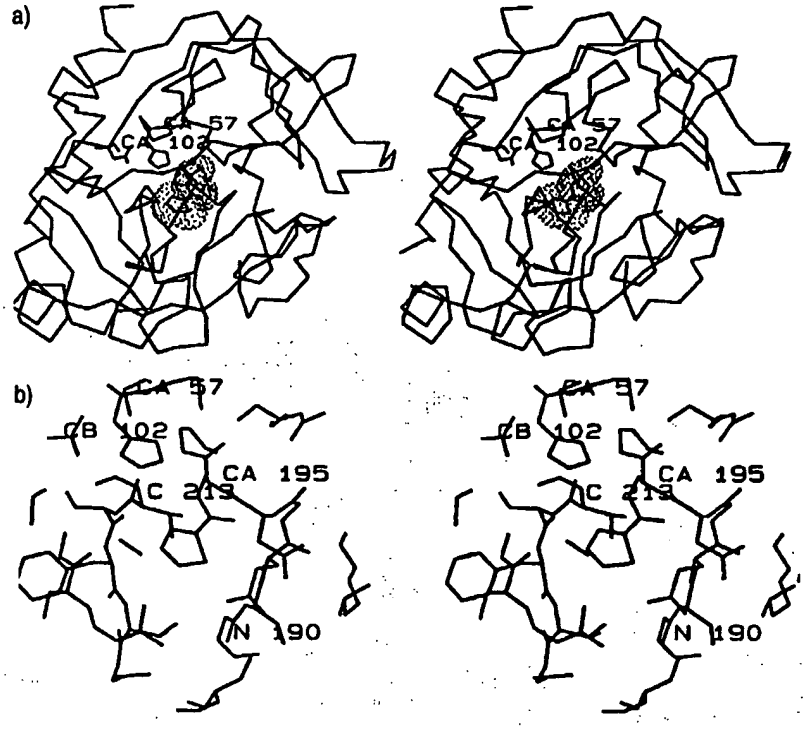

Fig. 3. – a) Cα backbone of porcine pancreatic elastase in its complex with the inhibitor YS3025 [13]. Only the acylating group of the inhibitor is shown (shaded and covalently linked to the enzyme Ser195 residue) together with the proteinase His57 and Asp102 catalytic residues. b) Close view of the active site of the YS3025-inhibited porcine pancreatic elastase, showing most of the enzyme amino acid residues forming the catalytic centre and involved in the inhibitor recognition [13]. The acylated Ser195 residue is in the central part of the picture. The elastase S_1 specificity subsite can be recognized as the central-lower pocket (of apolar nature) toward which the inhibitor thiophene ring is pointing.

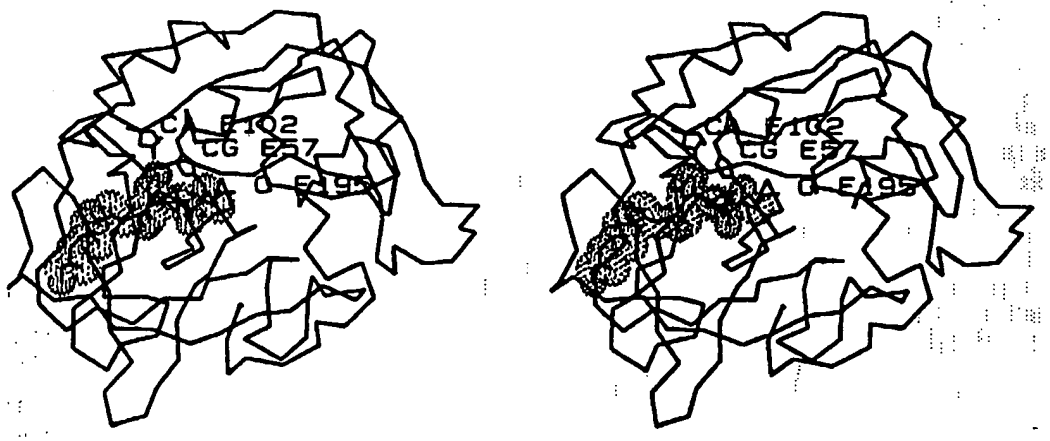

Fig. 4. – Binding mode of methoxysuccinyl-Ala-Ala-Pro-Ala-chloromethylketone to the active site of HLE [26]. Notice the position of the inhibitor P_1 Ala residue in the proteinase S_1 pocket (the polypeptide inhibitor is shaded).

the carbonyl group of residue P_1 is in a tetrahedral hemiketal configuration. The Ala-Ala-Pro-Ala(Val) substructure occupies the enzyme S_4-S_1 central region in an extended conformation (fig. 4). In particular, the methoxysuccinyl-Ala-Ala-Pro-Ala(Val) segment is strongly reminiscent in its conformation, as well as in the hydrogen bond network achieved with HLE, of the polypeptide geometry observed for the P_4-P_1 residues of OMTKY3, once bound to HLE [17, 18, 23]. As expected, the Ala(Val) P_1 residue of the inhibitor is sitting in the serine proteinase S_1 primary specificity pocket.

Conclusions

Although the structural information directly available on inhibitor:HLE interactions is not as extensive as in other enzymes belonging to the chymotrypsin superfamily [14, 15], our knowledge on HLE molecular properties is supported by several studies conducted on homologous serine proteinases (for review see [14, 17]). The detailed description of the active center of HLE [17, 18, 26] allows the design of powerful inhibitors. The synthesis of such compounds is also based on parallel studies of inhibitors specifically reacting at the active centre of the HLE homologous proteinase from porcine pancreas. Thus, several classes of low molecular weight compounds, such as modified peptide inhibitors, benzoxazinone-, isocoumarin- and cephalosporin-derivatives [19, 27, 28], are potentially available for experimentation on HLE.

Analysis of the structure and inhibition mechanism of protein HLE inhibitors, such as OMTKY3, makes it possible to extract only some overall information for the design of small, non-antigenic, synthetic inhibitors. In fact, protein proteinase inhibitor activity is based on the concurrent action of several factors, such as the complete exclusion of (re)active site residues from contact with the solvent, which can hardly be achieved by inhibitor molecules of a small size. Moreover, a substantial level of structural rigidity has to be coded into a polypeptide inhibitor molecule, in order to resist the hydrolytic action of the active catalytic triad.

The comparative study of several protein inhibitors active against serine proteinases belonging to the chymotrypsin superfamily has underlined the fact that additional contributions to the stabilisation of the E:I complex (*i.e.* to the inhibitory action) may be derived from the entropy gain recovered on removal of water molecules hydrogen bonded to the contact surfaces of the two interacting (macro)molecules. Moreover, the van der Waals interactions achieved at the molecular contacting surfaces (of several hundred $Å^2$ in protein inhibitors) allow the stabilization of the non-covalent E:I complex, relative to the free species, of a substantial amount. Most of these molecular features and properties can hardly be coded in the synthesis of low molecular weight inhibitors, which must therefore rely on extensive modifications of the physicochemical principles selected for HLE inhibition by natural protein inhibitors. In this respect, polypeptide loops of 20–30 amino acid residues, based on the molecular scaffolding of eglin c reactive site [25], or of squash seed inhibitor I [23], stabilised by chemical cross links or disulphide bridge(s), may prove to be effective synthetic inhibitors of HLE, displaying the advantages of macromolecular protein inhibitors, without eliciting the immune response after prolonged administration.

Acknowledgements: The authors wish to thank M. Luisetti, from IRCCS San Matteo, Pavia, for helpful suggestions and discussion during preparation of the manuscript.

References

1. Hörn H, Heidland A. – *In*: Proteases: Potential Role in Health and Diseases. New York and London, Plenum Press, 1982.
2. Barrett AJ, Salvesen G, (eds). – *In*: Proteinase Inhibitors. Amsterdam, New York and Oxford, Elsevier, 1986.
3. Cunningham DD, Long GL, (eds). – *In*: Proteinases in Biological Control and Biotechnology. New York, Alan R. Liss Inc., 1987.
4. Powers JC, Bengali ZH. – Elastase inhibitors for treatment of emphysema. *Am Rev Respir Dis* 1986; 134: 1097–1100.
5. Travis J, Fritz H. – Potential problems in designing elastase inhibitors for therapy. *Am Rev Respir Dis* 1991; 143: 1412–1415.
6. Grassi G, Travis J, Casali L, Luisetti M, (eds). – *In*: Biochemistry of Pulmonary Emphysema. London, Springer-Verlag, and Bi & Gi, Verona, 1992.
7. Janoff A. – Elastase in tissue injury. *Annu Rev Med* 1985; 36: 207–216.
8. Mechan R, (ed). – *In*: Regulation of Matrix Accumulation. New York, Academic Press, 1986.
9. Hutchens T, (ed). – *In*: Protein Recognition of Immobilized Ligands. New York, Alan R. Liss Inc., 1989.
10. Luisetti M, Piccioni PD, Donnini M, Peona V, Pozzi E, Grassi C. – Studies of MR889: a new synthetic proteinase inhibitor. *Biochem Biophys Res Commun* 1989; 165: 568–573.
11. Baici A, Pelloso R, Hörler D. – The kinetic mechanism of inhibition of human leukocyte elastase by MR889, a new cyclic thiolic compound. *Biochem Pharmacol* 1990; 39: 919–924.
12. Rizzi M, Casale E, Coda A, *et al.* – Serine proteinase inhibition by the cyclic thiolic compound YS3025: a crystallographic study. *Biochem Int* 1992; 28: 385–392.
13. Djinović-Carugo K, Rizzi M, *et al.* – Inhibition of serine proteinases belonging to the chymotrypsin superfamily by the cyclic thiolic compound YS3025: a comparative crystallographic study. *Biochem Biophys Res Commun* 1993; 193: 32–39.
14. Bode W, Huber R. – Natural protein proteinase inhibitors and their interaction with proteinases. *Eur J Biochem* 1992; 204: 433–451.
15. Bernstein FC, Koetzle TF, Williams GJB, *et al.* – The protein data bank: a computer-based archival file for macromolecular structures. *J Mol Biol* 1977; 112: 535–542.
16. Greer J. – Comparative modeling methods: application to the family of mammalian serine proteinases. *Proteins* 1990; 7: 317–334.
17. Bode W, Wei A-Z, Huber R, Meyer EF Jr, Travis J, Neumann S. – X-ray crystal structure of the complex of human leukocyte elastase (PMN elastase) and the third domain of turkey ovomucoid inhibitor. *EMBO J* 1986; 5: 2453–2458.
18. Wei A-Z, Mayr I, Bode W. – The refined 2.3 Å crystal structure of human leukocyte elastase in a complex with a valine chloromethylketone inhibitor. *FEBS Lett* 1988; 234: 367–373.

19. Navia MA, Springer JP, Lin T-Y, *et al.* – Crystallographic study of a β-lactam inhibitor complex with elastase at 1.84 Å resolution. *Nature (Lond)* 1987; 327: 79–82.
20. Laskowski M Jr, Kato I. – Protein inhibitors of proteinases. *Annu Rev Biochem* 1980; 49: 593–626.
21. Ascenzi P, Amiconi G, Bolognesi M, Onesti S, Petruzzelli R, Menegatti E. – Binding of the bovine and porcine pancreatic secretory trypsin inhibitor (Kazal) to human leukocyte elastase: a thermodynamic study. *J Enzyme Inhibition* 1991; 5: 207–213.
22. Schechter I, Berger A. – On the size of the active site in proteases: I. Papain. *Biochem Biophys Res Commun* 1967; 27: 157–162.
23. Bode W, Meyer E Jr, Powers JC. – Human leukocyte and porcine pancreatic elastase: X-ray crystal structures, mechanism, substrate specificity and mechanism-based inhibitors. *Biochemistry* 1989; 28: 1951–1963.
24. Bolognesi M, Gatti G, Menegatti E, *et al.* – Three-dimensional structure of the complex between pancreatic secretory trypsin inhibitor (Kazal type) and trypsinogen at 1.8 Å resolution. *J Mol Biol* 1982; 162: 839–868.
25. Frigerio F, Coda A, Puglese L, *et al.* – Crystal and molecular structure of the bovine α-chymotrypsin-eglin c complex at 2.0 Å resolution. *J Mol Biol* 1992; 225: 107–123.
26. Navia MA, McKeever BM, Springer JP, *et al.* – Structure of human neutrophil elastase in complex with a peptide chloromethylketone inhibitor at 1.84 Å resolution. *Proc Natl Acad Sci USA* 1989; 86: 7–11.
27. Meyer EF Jr, Cole G, Radhakrishnan R, Epp O. – Structure of native porcine pancreatic elastase at 1.65 Å resolution. *Acta Crystallogr* 1988; B44: 26–38.
28. Radhakrishnan R, Presta LG, Meyer EF Jr, Wildonger R. – Crystal structures of the complex of porcine pancreatic elastase with two valine-derived benzoxazinone inhibitors. *J Mol Biol* 1987; 198: 417–424.

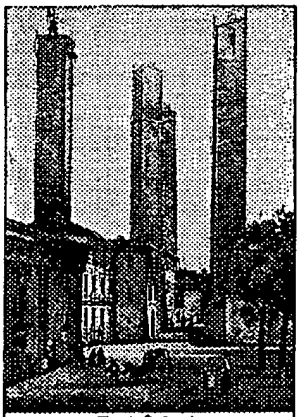

Torri di Pavia

STIC-ILL

BT - Microfilm
RC681.A1 A57137

From: Chen, Shin-Lin
Sent: Thursday, January 20, 2000 7:34 AM
To: STIC-ILL
Subject: articles

Please provide the following articles by 1-24-00. Thanks!
Serial No. 09/258,217.

1. Bizbiz et al., Atherosclerosis, 1997 (May), 131(1), p. 73-78.

2. Bolobnesi et al., Monaldi Archives for Chest Disease, 1994 (April), 49 (2), 144-149.

3. Maruyama et al., Am. J. Physiol., 1991, 261 (6, pt.2), H1716-H1726.

Ilkiw et al., Circulation Research, 1989 (April), 64 (4), p. 814-825.

Shin-Lin Chen
AU 1633
CM1 12E03
(703)305-1678

SC-39026, a Serine Elastase Inhibitor, Prevents Muscularization of Peripheral Arteries, Suggesting a Mechanism of Monocrotaline-Induced Pulmonary Hypertension in Rats

Roma Ilkiw, Livia Todorovich-Hunter, Kazuo Maruyama, John Shin, and Marlene Rabinovitch

In rats injected with the toxin monocrotaline, altered synthesis and distribution of pulmonary artery elastin suggest that increased elastase activity may be important in the development of vascular changes and progressive pulmonary hypertension. To test this hypothesis, male Sprague-Dawley rats (250–300 g) were given 40 mg/kg of the elastase inhibitor SC-39026 in a carboxymethylcellulose vehicle or vehicle only by gavage, 12 hours before and twice daily for 8 days after a single subcutaneous injection of either monocrotaline (60 mg/kg) or saline. Thirteen days after injection, indwelling cardiovascular catheters were inserted under pentobarbital anesthesia, and at 15 days after injection, pulmonary and systemic hemodynamic measurements were recorded with the animals awake. At post-mortem examination, the lungs were perfused and morphometric techniques applied for light and electron microscopic evaluation. Saline-injected rats given either SC-39026 or vehicle were similar in all features assessed. In contrast, monocrotaline-injected rats given SC-39026 had significantly lower mean pulmonary artery pressure than those given vehicle (21.0±1.6 vs. 27.5±0.8 mm Hg, $p<0.05$), and this correlated with a significant reduction in the number of abnormally muscularized arteries at alveolar wall level ($r^2=0.89$, $p<0.001$). SC-39026 did not significantly reduce monocrotaline-induced medial hypertrophy of muscular arteries, endothelial injury, and associated subendothelial edema; nor was there a significant increase in the proportion of the medial elastin, although a trend was apparent. Additional groups of monocrotaline injected rats were followed 3 weeks after injection, but both SC-39026 and vehicle-treated rats were similar at this point. Our data suggest that increased serine elastase activity associated with endothelial injury may mediate early abnormal pulmonary vascular smooth muscle differentiation resulting in muscularization of normally nonmuscular peripheral arteries and pulmonary hypertension induced in rats by injection of the toxin monocrotaline. Lack of persistence of this protective effect suggests that there may be continued elastase activity in this model. Failure to inhibit medial hypertrophy with SC-39026 suggests that a different mechanism or a different elastase may be involved in this structural change. (*Circulation Research* 1989;64:814–825)

Pulmonary hypertension, regardless of etiology, is associated with muscularization of normally nonmuscular peripheral arteries and with increased wall thickness of muscular arteries.[1] This is due to smooth muscle differentiation from precursor cells,[2] smooth muscle hypertrophy and/or

From the Departments of Cardiology and Pathology and the Research Institute, The Hospital for Sick Children, and from the Departments of Pediatrics and Pathology, University of Toronto, Toronto, Ontario, Canada.

Supported by Grant #T-724 from The Heart and Stroke Foundation of Ontario and by the Alberta Heritage Foundation. R.I. was a Research Fellow of the Alberta Heart Foundation and is currently a Research Fellow in the Department of Pediatric Cardiology at Texas Children's Hospital, Baylor College of Medicine, Houston, Texas. L.T.-H. received a graduate student stipend from the Canadian Heart Foundation. K.M. was supported by a fellowship from the Medical Research Council of Canada. J.S. was awarded the John D. Schultz Summer Studentship by The Heart and Stroke Foundation of Ontario, and M.R. is a Research Associate of The Heart and Stroke Foundation of Ontario.

Address for correspondence: Marlene Rabinovitch, MD, Department of Cardiology, The Hospital for Sick Children, 555 University Avenue, Toronto, Ontario (M5G1X8), Canada.

Received November 10, 1987; accepted September 28, 1988.

hyperplasia,[3,4] and progressive increases in collagen and elastin synthesis and accumulation in the media.[3,5–7] Structural and biochemical studies in our laboratory in which the toxin monocrotaline was used to induce pulmonary hypertension in rats, suggest that increased elastase activity may initiate and contribute to the progression of these vascular changes.[6,7] Fragmentation of the internal elastic lamina is noted as early as 4 days after injection of monocrotaline[7] and precedes the muscularization of peripheral arteries observed at day 8 and the rise in pulmonary artery pressure and resistance observed at day 12.[8] Continued elastase activity is suggested both by an increase in elastin synthesis out of proportion to elastin accumulation and by abnormal distribution of the medial elastin as interlamellar islands rather than as thicker elastic laminae, features observed at day 28 after monocrotaline injection.[6]

While previous investigators have shown that inhibitors of collagen synthesis are effective in reducing right ventricular and medial hypertrophy,[9,10] the intention of the present study was to explore the hypothesis that proteolytic, in particular elastolytic activity, induced by the toxin monocrotaline, may be initiating the neomuscularization of peripheral arteries, the medial thickening of the more proximal muscular arteries, and the associated increased connective tissue protein synthesis. We administered an elastase inhibitor, SC-39026 (Searle Pharmaceuticals, Skokie, Illinois)[11] and assessed whether this decreased or prevented the development of the above vascular changes. SC-39026 is a new agent, a 2-chloro-4-(1-hydroxyoctadecyl) benzoic acid, which inhibits neutrophil serine elastase.[11] The latter is a proteinase that degrades type IV collagen as well as elastin.[12] We hypothesized that since alterations in type IV collagen and other basement membrane proteins may be associated with changes in cell phenotype,[13,14] increased elastase activity in normally nonmuscular peripheral arteries might lead to differentiation of precursor cells (pericytes and intermediate cells) to mature smooth muscle.[2] Moreover, increased elastase activity in the vessel wall could also stimulate elastin synthesis and smooth muscle hypertrophy as has been suggested in vitro.[15] Neutrophil sequestration in the lung occurs within the first few hours after monocrotaline injection,[16] and while its role in the pathogenesis of vascular disease is questionable, it may be the source of increased elastase activity in rats.

We assessed the development of pulmonary hypertension in the rats by implanting indwelling cardiovascular catheters. Structural changes in the peripheral and hilar arteries, previously observed following monocrotaline injection, were analyzed by morphometric techniques. Muscularization of normally nonmuscular peripheral arteries (i.e. "extension of muscle") and medial hypertrophy of normally muscular arteries were assessed by light microscopy. Increased medial thickness of the hilar pulmonary artery as well as endothelial injury, subendothelial edema and the proportion of elastin in the media were evaluated by transmission electron microscopy.

Materials and Methods

Study Design

Pathogen-free male Sprague-Dawley rats (250–300 g) were used. Half were assigned at random to be given a single subcutaneous injection of monocrotaline (60 mg/kg) and the other half received an equal volume of 0.9% saline. Monocrotaline solutions were prepared from the crystalline compound (Transworld Chemicals, Rockville, Maryland) as previously described.[6] Half of the rats in each group were further assigned at random to receive by gavage either the elastase inhibitor SC-39026 (40 mg/kg/dose) suspended in carboxymethylcellulose vehicle or an equal volume of vehicle only. Carboxymethylcellulose vehicle was prepared by dissolving 1 g of the compound (Sigma Chemical Co, St. Louis, Missouri) in 100 ml of warmed distilled water. The rats were gavaged twice daily starting 12 hours before and continuing for 8 days after the monocrotaline or saline injection to provide a "window" around day 4. This was the time monocrotaline-induced increased elastase activity was first suspected on the basis of what appeared to be increased fragmentation of the internal elastic lamina of the hilar pulmonary artery.[7]

On day 13, after the monocrotaline or saline injection, the rats were anesthetized by an intraperitoneal injection of sodium pentobarbital (33 mg/kg), and indwelling catheters were inserted into the abdominal aorta under direct vision[17] and into the pulmonary artery by a modification[18] of a closed-chest technique previously described.[19] Pressure measurements and cardiac output were recorded 48 hours later to allow sufficient time for recovery from the effects of anesthesia. The heart and lungs were then prepared for morphological assessments.[18,20,21] Day 15 was chosen for physiological and morphological studies of the pulmonary vasculature to assure that satisfactory end-points would be obtained. This allowed for a few days beyond the time after monocrotaline injection, when a significant increase in pulmonary artery pressure and muscularization of peripheral arteries was previously observed.[8] Throughout the experimental period, food and water were supplied ad libitum. The number of rats with complete hemodynamic and morphologic data in each of the groups is indicated in the tables and figures.

To assess whether the results observed 2 weeks after monocrotaline injection in rats treated with SC-39026 were persistent at 3 weeks, a limited study was carried out. We assessed two groups of rats injected with monocrotaline, one treated with SC-39026, the other treated with vehicle as in the previously described protocol. Assessment of hemodynamic and morphological features of the heart

and lungs were carried out as in the previous groups with the exception that ultrastructural analyses were not performed.

Hemodynamic Measurements

Pressures were recorded from the pulmonary artery and aorta using physiological transducers (MS20, Electromedics, Englewood, Colorado) and an electrostatic recorder (ES1000, Gould, Cleveland, Ohio). Blood samples, 0.5 ml each, were obtained from the pulmonary and aortic catheters and blood gases were analyzed (Corning Glass Works, Medfield, Massachusetts); the hematocrit was determined from an additional 0.1-ml sample drawn from the aortic catheter. Oxygen consumption was measured as previously described,[18,20] with adjustments made for temperature and pressure and the cardiac output was calculated by the Fick principle using an oxygen carrying capacity derived from the measured hematocrit.

Tissue Preparation for Morphological Assessment

After the hemodynamic measurements were obtained, the rats were weighed and then anesthetized with an intraperitoneal injection of sodium pentobarbital (33 mg/kg). The animals were ventilated (Rodent Ventilator Model 683, Harvard Apparatus, South Natick, Massachusetts) through a tracheostomy at a rate of 75 breaths per minute and a stroke volume of 3.5 ml. The heart and lungs were then exposed via a median sternotomy. Heparin (500 units) was injected into the right ventricle and allowed to circulate for 2 minutes. The central pulmonary artery was cannulated with a 5-cm length of polyethylene tubing (PE 90, i.d. 0.86×o.d. 1.27 mm) through a right ventriculotomy incision and then perfused with preheated (37° C), heparinized (0.5% vol/vol) phosphate-buffered saline at 20 cm water pressure for 5 minutes to clear the lungs of blood. The left pulmonary artery was then temporarily occluded, and the left lung was covered in a small plastic bag to avoid fixation while the right lung was perfused at the pressure measured in vivo, for 10 minutes with a cold (4° C), 1% glutaraldehyde in 4% formaldehyde solution. The right pulmonary artery was then occluded, the lung was removed, and a block of tissue, approximately 5×5×2 mm, containing the hilar pulmonary artery was then taken. The tissue was diced into small blocks approximately 1×1×2 mm, fixed for 1 more hour, and then placed in 0.1 M phosphate buffer and processed for transmission electron microscopy.

The left pulmonary artery was then unclamped and injected with a hot (60° C), radiopaque barium-gelatin mixture at 100 cm water pressure for 5 minutes, and then clamped. The lung was distended through the trachea with 10% formaldehyde at 36 cm water pressure and perfused continuously for 3 days. A block of tissue 10×10×5 mm was obtained from the midsection of the lung for light microscopic analysis.[18,20] The right ventricle (RV) of the heart was dissected from the left ventricle plus septum (LV+S) and weighed separately.[21] Ventricular weights were expressed as the ratio RV/(LV+S) and also as the ratio of the weight of the RV to final body weight (FBW).

Light Microscopic Analysis

Lung tissue for histological evaluation was embedded in paraffin and stained by the elastic Van Gieson method. Slides were analyzed without knowledge of treatment group. Using previously described morphometric techniques,[18,20] all barium-filled arteries in each tissue section were analyzed at ×400 magnification, for an average of 97 arteries per section (range, 81–120). Each artery was first "landmarked" according to its accompanying airway, as being either preacinar or related to a terminal bronchiolus, respiratory bronchiolus, alveolar duct, or alveolar wall, and its external diameter was measured. Each artery was further described as being either muscular (with a complete medial muscular coat), partially muscular (with an incomplete coat), or nonmuscular (no muscle apparent). Extension of muscle into peripheral, normally nonmuscular arteries was evaluated by the percentage of muscular and partially muscular arteries at each airway level. Medial wall thickness, an index of medial hypertrophy, was calculated for each muscular and partially muscular artery as a percent wall thickness (%WT).[18,20] For each rat, an average wall thickness for arteries of the various sizes (50–99 and 100–149 μm) was calculated. In each of 10 consecutive fields at × 250 magnification, all alveoli and arteries were counted. Arterial density was expressed as the number of arteries per 100 alveoli.

Transmission Electron Microscopic Analysis

Tissue blocks were dehydrated and embedded in Epon, from which thin sections (1 μm) were cut and stained with toluidine blue. Blocks containing the hilar pulmonary artery were cut into ultrathin sections (600–900 Å), prepared on copper grids, stained with 5% uranyl acetate and 0.4% lead citrate, and viewed in a transmission electron microscope (model 201, Philips Electronic Instruments, Mount Vernon, New York). For each animal, at least three consecutive photomicrographs that included the full thickness of the hilar artery were taken at ×3,600 magnification for measurement of wall thickness as well as assessment of the thickness of elastic laminae of the media. Similarly, for each animal, at least eight consecutive photomicrographs that included the intima were taken at ×17,500 magnification for assessment of endothelial cell morphology, width of subendothelial space, and thickness of internal elastic lamina. Photomicrographs were printed in 20×20 cm format and analyzed with a semiautomatic computerized system (Interactive Image Analysis System IBAS-1, Zeiss, Thornwood, New York).

The intima of the hilar pulmonary artery was examined for evidence of monocrotaline-induced

TABLE 1. Final Body Weight, Hematocrit, Cardiac Output, Arterial Blood Gas Values, Systemic Arterial Pressure 2 Weeks After Injection

GP	(*n*)	FBW (g)	Hct (%)	Co (ml/min/kg)	Pa_{O_2} (mm Hg)	Pa_{CO_2} (mm Hg)	pH	Psa (mm Hg)
M/V	(10)	223±3	0.42±0.01	871±68	82±2	33±1	7.44±0.01	116±3
M/SC-I	(9)	219±5 *	0.40±0.01	836±125	84±3	32±1	7.46±0.01	115±4
S/V	(7)	251±5	0.43±0.01	856±60	84±3	33±1	7.46±0.02	117±4
S/SC-I	(7)	254±3	0.42±0.01	846±51	86±2	32±1	7.47±0.01	118±3

GP, group; *n*, number; FBW, final body weight; Hct, hematocrit; CO, cardiac output; Psa, mean systemic arterial pressure; M/V and M/SC-I, monocrotaline-injected rats treated with vehicle and SC-39026 inhibitor, respectively; S/V and S/SC-I, saline-injected rats treated with vehicle and SC-39026 inhibitor, respectively. Values are mean±SEM. *$p<0.001$, saline compared with monocrotaline.

changes. Ten consecutive endothelial cells per artery were assessed, and the number showing evidence of injury (i.e., vacuolation, pallor, and foamy cytoplasm) was recorded and expressed as a percent of injured endothelial cells per artery. The subendothelium, defined as the region between the adlumenal edge of the endothelium and the adlumenal border of the internal elastic lamina, was examined for evidence of edema by measuring its thickness at three equidistant points on each print. Thus, at least 24 measurements were recorded per vessel and averaged. The thickness of the internal elastic lamina in each photomicrograph was derived from the digitized surface area, divided by the measured length; from eight assessments, an average thickness per artery was calculated.

The media was defined as the region between the ablumenal edge of the internal elastic lamina and the ablumenal border of external elastic lamina. The thickness of the media of the hilar artery was measured at three equidistant points on each of the photomicrographs, and an average thickness was calculated for each vessel. The sum of the digitized surface areas of all the elastic laminae in the media was calculated and related to the digitized surface area of the media. Assessments from each of the prints taken from a given artery were averaged.

SC-39026 Plasma Levels

After completion of these studies, six additional weight-matched male Sprague-Dawley rats were gavaged with SC-39026 for 6 days. Just before the first dose and 9 hours after the last dose, 1 ml of tail vein blood was obtained, and plasma levels were determined by the Department of Drug Metabolism at Searle Research Laboratories, Skokie, Illinois, using a high-performance liquid chromatography assay. Values before gavage with SC-39026 ranged from 0.10 to 0.24 μg/ml (background activity), whereas levels 9 hours after the last dose were 0.30–0.38 μg/ml in two rats and 1.30–4.17 μg/ml in the remaining four. Since only values greater than 0.6 μg/ml are considered to represent a therapeutic level (Dr. G. Fuller, Searle, personal communication), it appears that there is considerable variation in the degree of absorption of the compound after oral administration in rats.

Analysis of Data

Two-way analysis of variance was used to compare the effects of monocrotaline and SC-39026 in the four groups: saline/vehicle, saline/SC-39026, monocrotaline/vehicle, and monocrotaline/SC-39026. When significant variance was found, Duncan's test of multiple comparisons was used to determine which groups were different.[22] Linear regression analysis was used to detect whether, in individual monocrotaline injected rats, there was a relation between the mean pulmonary artery pressure and structural and ultrastructural differences in the pulmonary arteries. This analysis was also applied to determine the relation between the amount of elastin in the vessel wall, the wall thickness of the pulmonary artery and the degree of muscularization of peripheral arteries. In the limited study carried out to assess differences in the SC-39026 treated and untreated monocrotaline injected rats at 3 weeks after injection, comparisons are based on a Student's *t* test. Differences were considered statistically significant at $p<0.05$. Mean values±SEM are given in the figures and tables, and the number of rats assessed in each group is noted.

Results

Growth, Hemodynamic Measurements and Ventricular Weights at 2 Weeks

Complete data were obtained in 33 rats: seven saline/vehicle, seven saline/SC-39026, 10 monocrotaline/vehicle, and nine monocrotaline/SC-39026. Both saline/vehicle and saline/SC-39026 groups had similar final body weights. The monocrotaline groups had lower final weights than the saline rats ($p<0.001$, ANOVA), a feature not significantly altered by SC-39026. There were no significant differences between the four groups in hematocrit, cardiac output, arterial blood gas values, and systemic artery pressure (Table 1).

The mean pulmonary artery pressures of the saline/vehicle and saline/SC-39026 groups were similar, 16.4±1.1 and 17.4±0.9 mm Hg, respectively (Figure 1). The monocrotaline groups had signifi-

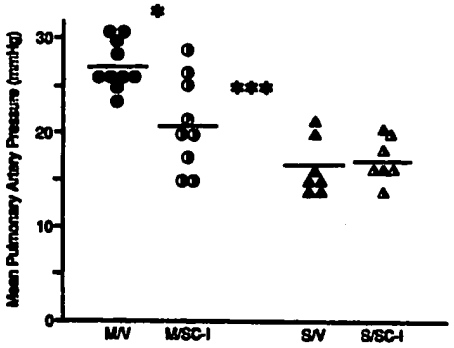

FIGURE 1. *Mean pulmonary artery pressure values in the four treatment groups. M, monocrotaline; V, vehicle; SC-I, elastase inhibitor SC-39026; S, saline. M/V (n=10). M/SC-I (n=9). S/V (n=7). S/SC-I (n=7). Data points represent pulmonary artery pressure value for each animal. Solid line denotes mean for the group. The M groups have significantly higher values than the S groups, ***p<0.001 (ANOVA). M/SC-I rats are significantly lower than M/V, *p<0.05 (Duncan's Multiple Range Test).*

cantly higher mean pulmonary artery pressure values compared with saline rats ($p<0.001$, ANOVA). However, while mean pulmonary artery pressure in the monocrotaline/vehicle group was 27.5±0.8 mm Hg, treatment of monocrotaline rats with SC-39026 resulted in significantly lower values (21.00±1.6 mm Hg, $p<0.05$, Duncan's Multiple Range Test). In five of nine rats in the monocrotaline/SC-39026 group, pulmonary artery pressure values were within the range of saline controls (Figure 1).

There was considerable overlap in RV/FBW as well as in the RV/(LV+S) values among the four groups. The saline/vehicle and saline/SC-39026 groups had similar values for RV/(LV+S) and RV/FBW. Monocrotaline injection resulted in higher values for RV/(LV+S) ($p<0.05$) and for RV/FBW ($p<0.001$)(ANOVA). Values for RV/FBW but not for RV/(LV+S) were, however, significantly lower in the monocrotaline/SC-39026 group than in the monocrotaline/vehicle group ($p<0.05$, Duncan's Multiple Range Test) (Table 2).

Light Microscopic Analysis at 2 Weeks

Light microscopic structural analysis of the peripheral pulmonary vasculature was performed on 25 of the 33 unselected rats: six saline/vehicle, six saline/SC-39026, six monocrotaline/vehicle, and seven monocrotaline/SC-39026.

Extension of muscle. Saline/vehicle and saline/SC-39026 rats had only a small percentage of arteries muscularized at the alveolar wall level (1.9±1.4 and 0.4±0.4%, respectively) (Figure 2). Monocrotaline-injected animals had significantly greater muscularization of alveolar wall and duct arteries, compared with saline rats ($p<0.001$ for both, ANOVA). The monocrotaline/vehicle group had 24.1±2.6% alveolar wall arteries muscularized. Treatment of monocrotaline-injected rats with SC-39026 resulted in a decreased percentage of alveolar wall arteries muscularized (10.0±3.6%, $p<0.05$, Duncan's Multiple Range Test). A trend toward a decreased percent of alveolar duct arteries muscularized was apparent, although the difference was not statistically significant. In the monocrotaline/vehicle rats, there was no significant correlation between the percent alveolar wall arteries muscularized and the level of mean pulmonary artery pressure. Values were high for both parameters. In the monocrotaline/SC-39026 group, however, there was a significant correlation between the level of pulmonary artery pressure and the percent of alveolar wall arteries muscularized ($r^2=0.89$, intercept=15.245, slope=0.599, 95% confidence limits of the slope=0.599±1.96, $p<0.001$) (Figure 3).

Medial wall thickness of muscular arteries. The saline/vehicle and saline/SC-39026 groups had similar values for medial wall thickness (%WT) of muscular arteries of 50–99 and 100–149 μm external diameter (Table 2). The monocrotaline-injected rats had significantly increased %WT compared with the saline-injected animals in arteries of 100–149 μm external diameter only ($p<0.001$, ANOVA). Treatment of the monocrotaline injected rats with SC-39026 did not result in a significantly decreased

TABLE 2. Assessments of Right Ventricular Hypertrophy and Light Microscopic Measurements of Medial Hypertrophy and Arterial Density 2 Weeks After Injection

GP	(n)	RV/FBW (g/kg)	RV/LV	% Wall thickness 50–99 μm	% Wall thickness 100–149 μm	Arterial density (arteries/100 alveoli)
M/V	(6)	0.61±0.03	0.26±0.01	3.85±0.21	4.12±0.32	4.62±0.28
M/SC-I	(7)	0.54±0.03* †	0.24±0.01 ‡	3.71±0.13	3.73±0.16 ‡	4.73±0.17
S/V	(6)	0.50±0.02	0.23±0.01	3.49±0.17	2.73±0.22	4.33±0.20
S/SC-I	(6)	0.52±0.02	0.23±0.01	3.45±0.07	2.49±0.06	4.68±0.22

GP, group; n, number; RV/FBW, ratio of right ventricular to final body weight; RV/LV, ratio of right ventricular weight to left ventricular+septal weight; M/V and M/SC-I, monocrotaline-injected rats treated with vehicle and SC-39026 inhibitor, respectively; S/V and S/SC-I, saline-injected rats treated with vehicle and SC-39026 inhibitor, respectively.

*$p<0.05$, M/V compared with M/SC-I.

†$p<0.05$, saline compared with monocrotaline.

‡$p<0.001$, saline compared with monocrotaline.

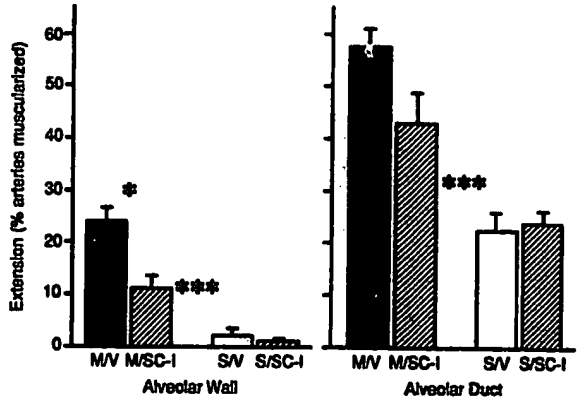

FIGURE 2. *Extension of Muscle: Percent of peripheral arteries muscularized at the alveolar wall and alveolar duct level. M, monocrotaline; V, vehicle; SC-I, elastase inhibitor SC-39026; S, saline. M/V* (n=6). *M/SC-I* (n=7). *S/V* (n=6). *S/SC-I* (n=6). *Values are mean±SEM for each group. M groups had abnormally increased muscularization of arteries at alveolar wall and alveolar duct level, compared with S groups,* ***$p<0.001$ *(ANOVA). The M/SC-I group compared with the M/V group had decreased muscularization at alveolar wall level,* *$p<0.05$ *(Duncan's Multiple Range Test) with a similar trend at alveolar duct level, although not statistically significant.*

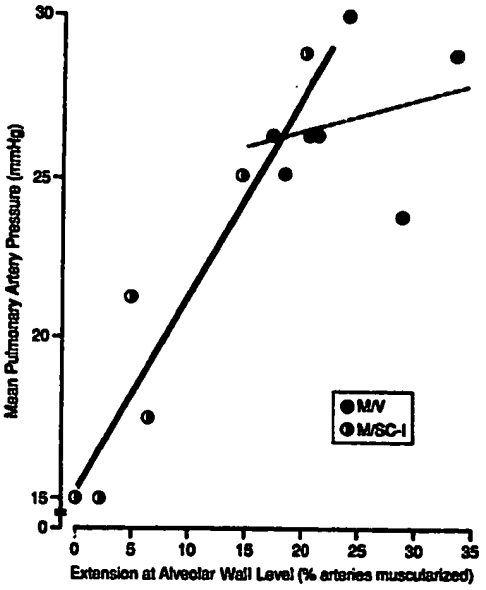

FIGURE 3. *Correlation of mean pulmonary artery pressure with extension of muscle into alveolar wall arteries. M, monocrotaline; V, vehicle; SC-I, elastase inhibitor SC-39026. M/V* (n=6). *M/SC-I* (n=7). *There is no significant correlation between the two measurements in M/V rats whereas in M/SC-I rats* $r^2=0.89$, *slope=15.245, intercept=0.599 (95% confidence limits=0.599±1.96),* $p<0.001$.

%WT, although there was a trend in that direction (Table 2).

Arterial density. There was no difference among the four groups in the number of arteries per 100 alveoli (Table 2). Lung volumes and absolute number of alveoli per mm^2 were also similar.

Ultrastructural Analysis at 2 Weeks

Ultrastructural analysis of the hilar pulmonary artery was performed on 18 of 33 unselected rats: three saline/vehicle, three saline/SC-39026, six monocrotaline/vehicle, and six monocrotaline/SC-39026.

Intima. Both saline/vehicle and saline/SC-39026 groups had few injured endothelial cells per artery and a barely measurable subendothelial space (Figures 4 and 5). In contrast, monocrotaline-injected animals had a high proportion of injured endothelial cells per artery and evidence of subendothelial edema judged by a wide subendothelial space ($p<0.001$, ANOVA for both comparisons). Treatment of monocrotaline rats with SC-39026 did not

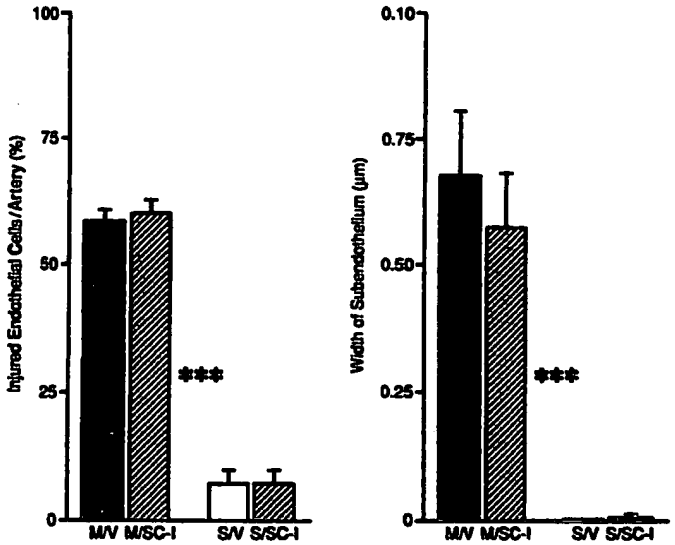

FIGURE 4. *Ultrastructural features of the intima of hilar pulmonary arteries (endothelium and subendothelial space). M, monocrotaline; V, vehicle; SC-I, elastase inhibitor SC-39026; S, saline. M/V* (n=6). *M/SC-I* (n=6). *S/V* (n=3). *S/SC-I* (n=3). *Values are mean±SEM for each group. The number of 'injured' endothelial cells per artery as defined in the text and the width of the subendothelial space is increased in M groups,* ***$p<0.001$ *for both (ANOVA). No significant differences exist between M/V and M/SC-I groups.*

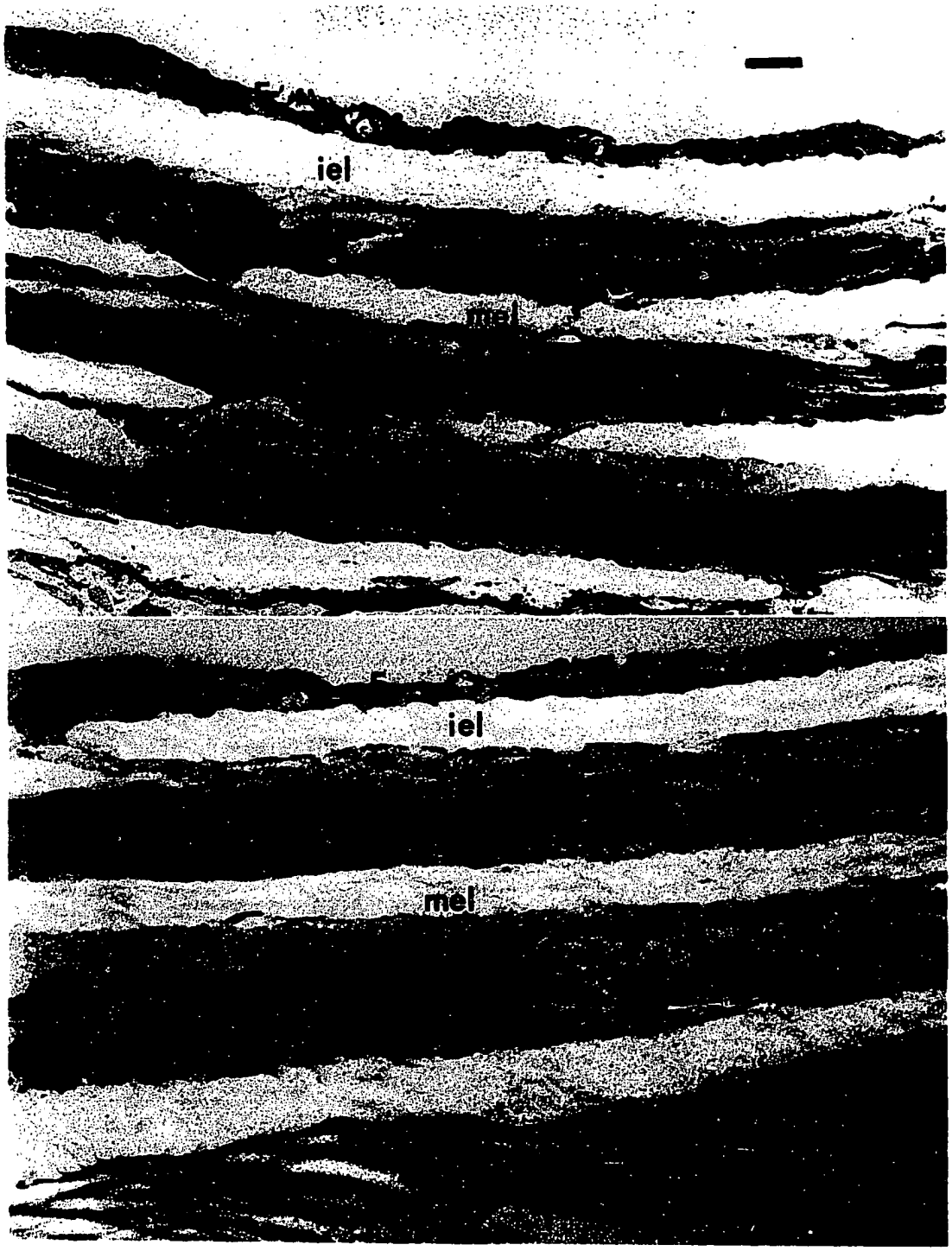
iel
mel
iel
mel

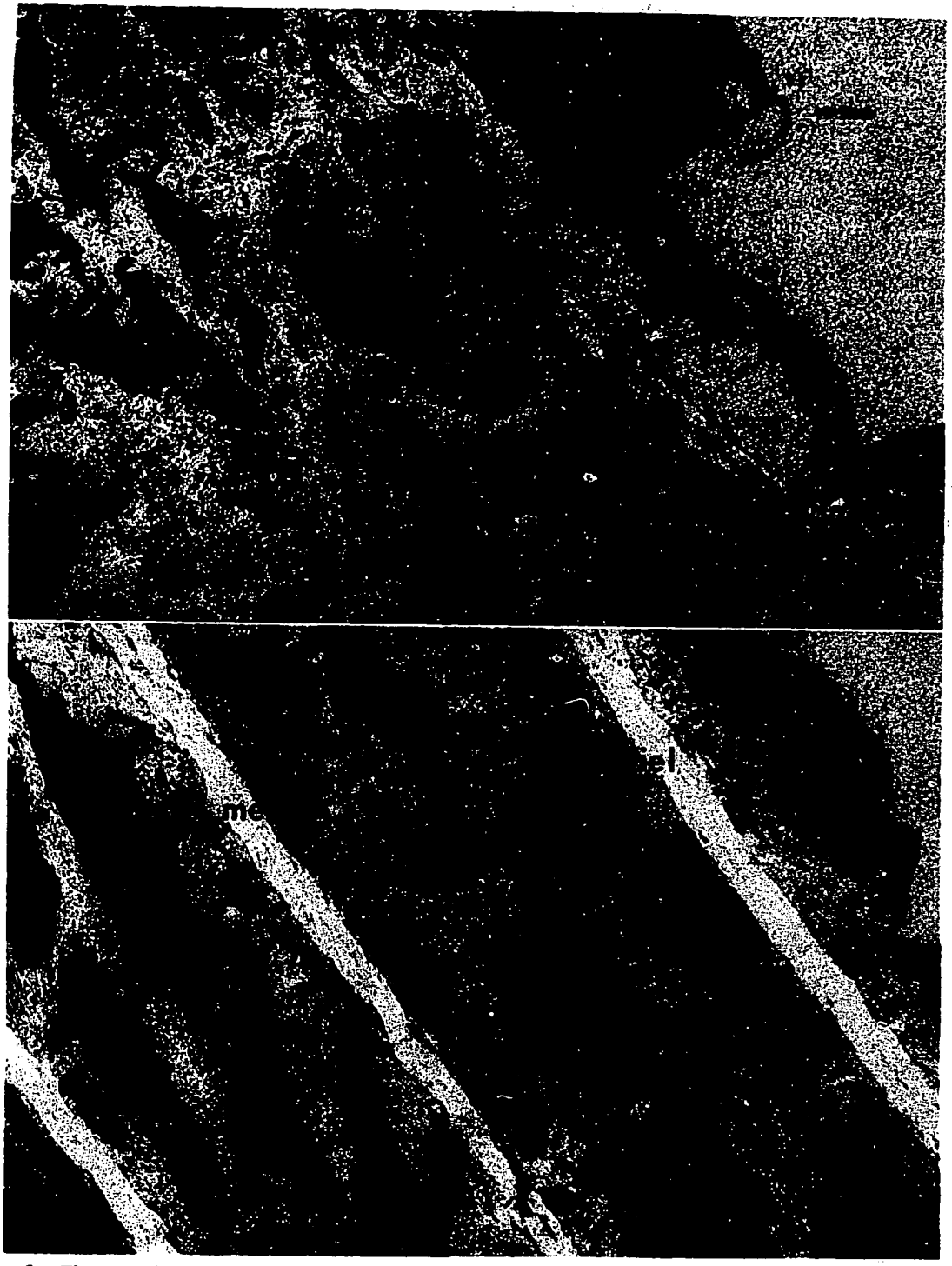

FIGURE 5. ***Electron photomicrographs of the hilar pulmonary arteries. A saline/vehicle rat*** **(top left)** ***and a saline/SC-39026 rat*** **(bottom left)** ***show normal endothelial (E) cells and virtually no subendothelial (S) space. In contrast, endothelial cells in the hilar pulmonary artery of a monocrotaline/vehicle*** **(top right)** ***and a monocrotaline/SC-39026*** **(bottom right)** ***rat show considerable swelling and pallor, with well-defined subendothelial space. SM, smooth muscle cell. Thickness of internal elastic lamina (iel) is similar in all photomicrographs, but the proportion of media occupied by elastic laminae (mel) is reduced in the photomicrographs from the monocrotaline rats*** **(top and bottom right).** ***Magnification, ×6,138; bar, 1.5 μm.***

alter the severity of these abnormalities. The width of the internal elastic lamina was similar in saline and monocrotaline-injected rats and was unaffected by SC-39026 (Figure 6).

Media. The thickness of the media of the hilar pulmonary artery was similar in both saline groups (Figure 7), but in monocrotaline injected rats, it was increased ($p<0.01$, ANOVA). Values in monocrotaline/SC-39026 and monocrotaline/vehicle groups were similar. The ratio of the surface area of the elastic laminae of the media to the surface area of the media was similar for saline/vehicle and saline/SC-39026 rats but was decreased in the monocrotaline groups ($p<0.001$, ANOVA). Moreover, qualitatively, the elastic laminae appeared fragmented (Figure 4). Treatment of monocrotaline-injected rats with SC-39026 did not result in a significantly increased proportion of media occupied by elastic laminae, although a trend was apparent (Figures 4 and 6) and the laminae appeared less fragmented (Figure 4). In individual monocrotaline-injected animals, the proportion of elastic laminae in the media did not correlate significantly with the thickness of the media or the mean pulmonary artery pressure.

Hemodynamic and Structural Changes at 3 Weeks.

At 3 weeks after monocrotaline injection, maintaining catheters in the pulmonary artery of the rats was particularly difficult because they tended to flip out, probably because of the very high levels of pulmonary artery pressure. This phenomenon has been previously described.[23] We were therefore able to compare only four SC-39026 and four vehicle-treated monocrotaline-injected rats with respect to pressures, but eight and 12 rats, respectively, with regard to right ventricular hypertrophy. Light microscopic morphometric assessment was carried out on the eight rats in which pressures were obtained. At the 3-week time point, there were no significant differences in the two groups with respect to pulmonary artery pressure, cardiac output, and right ventricular hypertrophy expressed either as the ratio of right to left ventricular weight or as the ratio of right ventricular to body weight, nor was there a significant difference in the degree of muscularization of peripheral arteries or in the medial wall thickness of normally muscular arteries (Table 3).

Discussion

We have previously reported that in rats, injury to the pulmonary vascular endothelium by the pyrrolizidine alkaloid metabolite of monocrotaline precedes muscularization of the normally nonmuscular distal pulmonary vascular bed and the rise in pulmonary artery pressure and increase in pulmonary vascular reactivity.[8] That muscularization of distal vessels precedes pulmonary hypertension was also evident in studies by Meyrick et al, in which rats were fed *Crotalaria spectabilis* seeds.[20] Since administration of the elastase inhibitor SC-39026 for 7 days after injection of monocrotaline reduced extension of muscle into normally nonmuscular peripheral arteries correlating with a reduction in the severity of pulmonary hypertension at 2 weeks, our study supports the hypothesis that elastase activity may initiate this vascular change. Muscularization of peripheral arteries is thought to result from the differentiation of precursor cells (pericytes) to mature smooth muscle cells.[2] Cellular differentiation may be regulated by changes in basement membrane and other extracellular matrix proteins.[13,14] Thus, SC-39026 may have prevented muscularization of peripheral arteries by inhibiting degradation by elastase of elastin or type IV collagen, a basement membrane component, or by some other as yet undescribed antiproteolytic effect.

The reduction in pulmonary artery pressure was not related to a change in cardiac output, mean systemic arterial pressure, hematocrit or arterial oxygen tension. We report pulmonary artery pressure and not pulmonary vascular resistance as we did not record left ventricular end-diastolic pressure. However, we established that there was no significant change in cardiac output, and it has been observed previously by our group[8] and others[20] that there is no significant change in left ventricular end diastolic pressure after monocrotaline injection. For these reasons, the pulmonary artery pressure changes likely reflect similar alterations in pulmonary vascular resistance. In six of nine rats, the values of pulmonary artery pressure in the monocrotaline-injected rats treated with the inhibitor SC-39026 were similar to those in the saline injected controls, whereas in the other three rats, only a partial reduction in pulmonary hypertension may have been achieved. The variability in response may be due to the variation from rat to rat in the severity of monocrotaline-induced vascular damage or in the absorption characteristics of the orally administered SC-39026.[11] While the two may certainly interrelate, the relatively uniform response in the untreated monocrotaline injected rats and the variability in SC-39026 absorption demonstrated in a similarly treated group suggest that the latter may be a more likely explanation.

Associated with the decreased pulmonary artery pressure at 2 weeks in monocrotaline injected rats treated with SC-39026, right ventricular hypertrophy was less as judged by the ratio of right ventricle to final body weight. That there was only a trend toward a decrease in the ratio of right to left ventricular weights is due, most likely, to the considerable overlap in values even with saline injected rats.

In previous studies, we observed increased fragmentation of the internal elastic lamina of more proximal and larger muscular pulmonary arteries, at 4 days after injection of the toxin monocrotaline in association with endothelial damage.[7] This preceded the development of medial hypertrophy and the increase in elastin synthesis[6] observed 16 days after injection. We therefore hypothesized that increased elastase activity was also important in the

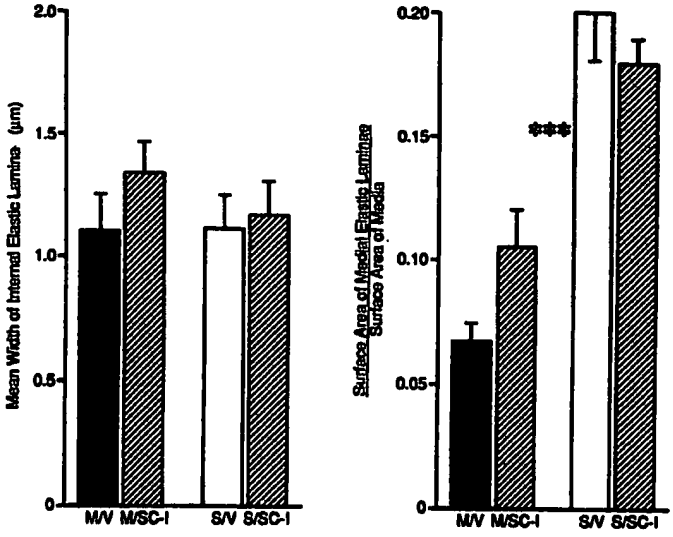

FIGURE 6. *Mean width of internal elastic lamina (iel) of hilar pulmonary arteries and proportion of medial elastic laminae. M, monocrotaline; V, vehicle; SC-I, elastase inhibitor SC-39026; S, saline. Values are mean±SEM for each group. There were no differences between the four groups in the mean width of the iel. Quantification of elastic laminae of the media of the four groups. M rats have a decreased proportion of medial elastin relative to S rats* ***$p<0.001$, *(ANOVA) and in M/SC-I (SC-39026), rats, there is a trend apparent toward a proportion similar to that in S rats. The numbers* (n) *in each group are given in Figure 4.*

pathogenesis of the increased medial wall thickness of more proximal normally muscular arteries. In the present study, however, we were unable to show a significant reduction in the severity of monocrotaline-induced medial hypertrophy with administration of the elastase inhibitor. We had anticipated that an increase in the proportion of elastic laminae in the media of the hilar pulmonary artery associated with a decrease in fragmentation might more sensitively reflect some degree of elastase inhibition. However, the difference comparing SC-39026 treated and non-treated monocrotaline-injected rats was small and statistically insignificant. Thus, it seemed that a different mechanism or elastase may be responsible for medial hypertrophy.

We wondered whether observation of the rats for 3 weeks after injection of the toxin monocrotaline might reveal a more pronounced effect of the inhibitor on medial hypertrophy and medial elastin. We did not, however, observe any significant difference in SC-39026 treated or untreated monocrotaline-injected rats. Moreover, the decrease in muscularization of peripheral arteries, pulmonary artery pressure, and right ventricular hypertrophy previously observed in SC-39026-treated rats at 2 weeks did not persist. It is possible that a higher or more constant level of inhibitor may be necessary to achieve a sustained response. This is currently being explored with the Searle company. We have not had success with an intravenous preparation because the compound crystallized (authors' unpublished observations), so a food-admix is now being prepared.

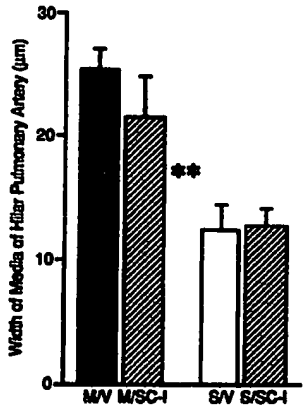

FIGURE 7. *Thickness of the media of the hilar pulmonary artery. M, monocrotaline; V, vehicle; SC-I, elastase inhibitor SC-39026; S, saline. Values are mean±SEM for each group. There is a significant difference between monocrotaline and saline groups,* **$p<0.01$ *(ANOVA). The numbers* (n) *in each group are given in Figure 4.*

The source of the elastase, which may be involved in the muscularization of distal vessels, is not known. Since the inhibitor is specific for neutrophil elastase one might speculate that the neutrophils observed early in the lung are the source, but their appearance is transient and it is questionable whether they are related to the pathogenesis of the vascular changes particularly since animals such as mice, that have the greatest inflammatory response to monocrotaline do not develop vascular changes.[24] The spectrum of elastase activity of vascular endothelial cells is not known,[25] and it is conceivable that, in response to the endothelial injury induced by monocrotaline, an elastase is released that would be inhibited by SC-39026. It has been shown that smooth muscle cells produce a serine elastase,[26] but it is not known whether it is inhibited by SC-39026.

While neutrophils are observed early and transiently in association with monocrotaline injection, the presence of platelets and microthrombi are even more evident, so platelet production of[27] or interaction with elastase[28] may be important. An increased number of alveolar macrophages,[29] are associated with the development and progression of monocrotaline-induced pulmonary hypertension, but they produce primarily metalloelastases.[30]

TABLE 3. Hemodynamic and Structural Measurements 3 Weeks after Injection of Monocrotaline

GP	(n)	Pressures PA	Pressures Ao	Arterial blood gasses pH	Arterial blood gasses Po_2	Arterial blood gasses Pco_2	Hematocrit (%)	Cardiac output (ml/kg/min)	(n)	FBW (g)	Right ventricular hypertrophy RV/LV	Right ventricular hypertrophy RV/FBW	(n)	Extension of muscle (%) Alveolar wall	Extension of muscle (%) Alveolar duct	Wall thickness (%) 50–100 μm
M/V	(4)	38±3	104±3	7.41±.02	81±3	33±2	40±.6	439±32	(8)	337±7	0.44±.03	0.93±.06	(4)	64±10	83±6	7.9±0.9
M/SC-I	(4)	53±8	98±4	7.44±.02	75±9	33±1	39±.4	405±45	(11)	325±7	0.45±.04	0.91±.08	(4)	59±11	86±6	7.6±3.0

GP, group; n, number; PA, pulmonary artery; Ao, aorta; FBW, final body weight; RV/LV, ratio of right ventricular weight to left ventricular+septal weight; M/V and M/SC-I, monocrotaline-injected rats treated with vehicle and SC-39026 inhibitor, respectively.

While our study suggests an antielastase effect of SC-39026, it is possible that this compound alters the metabolism of monocrotaline in such a way as to make it less toxic. This seems unlikely since the degree of endothelial injury and subendothelial swelling we observed was similar in the treated and untreated monocrotaline-injected rats. An increase in the activity of angiotensin converting enzyme (a serine protease) has been observed in association with an early phase of monocrotaline pulmonary toxicity,[31,32] but SC-39026 has been shown to not inhibit this enzyme.[11]

We conclude that we have evidence in the monocrotaline-injected rat model indicating that serine elastase may be associated with muscularization of peripheral arteries leading to the development of pulmonary hypertension. Further in vitro and immunocytochemical studies will be necessary to establish the mechanism whereby elastase activity in the small peripheral vessels leads to the differentiation of smooth muscle cells from precursor cells and especially whether this is related to degradation of the component of the basement membrane that is type IV collagen. Also, further studies will be necessary to show that the mechanism of induction of abnormal muscularization of peripheral arteries after monocrotaline is similar when chronic hypoxia is the stimulus or when this feature results from the high pulmonary blood flow and pressure produced by a congenital cardiac defect with a left-to-right shunt.[1]

Acknowledgments

The authors gratefully acknowledge the technical assistance of Ms. Nancy Boudreau in carrying out the hemodynamic studies; the secretarial assistance of Ms. Dianna Bereczki in preparing the manuscript; and Ms. Eva Struthers, Mr. Marc Rochon, Mr. Ray Caesar, Mr. Mike Starr, and Ms. Toni Bothwell for the illustrations. We are also grateful to Dr. George Fuller, Director of Research and Development at Searle Pharmaceuticals, and Dr. Dick Mueller, who developed the SC-39026 HPLC assay. SC-39026 was a gift of Dr. G. Fuller, Searle Pharmaceuticals, Skokie, Illinois.

References

1. Rabinovitch M: Pulmonary hypertension, in Adams FH, Emmanouilides GC (eds): *Moss' Heart Disease in Infants, Children and Adolescents*. Baltimore, Williams and Wilkins, ed 3, 1983, pp 669–692
2. Meyrick B, Reid L: Ultrastructural features of the distended pulmonary arteries of normal rats. *Anat Rec* 1979;193:71–93
3. Meyrick B, Reid L: The effect of continued hypoxia on rat pulmonary arterial circulation: An ultrastructural study. *Lab Invest* 1978;38:188–200
4. Meyrick B, Reid L: Hypoxia and incorporation of ^3H thymidine by cells of rat pulmonary arteries and alveolar wall. *Am J Pathol* 1979;96:51–70
5. Stenmark KR, Fasules J, Hyde DM, Voelkel NF, Henson J, Tucker A, Wilson H, Reeves JT: Severe pulmonary arterial hypertension and arterial adventitial changes in newborn calves at 4300 m. *J Appl Physiol* 1987;62:821–830
6. Todorovich L, Johnson D, Ranger P, Keeley F, Rabinovitch M: Altered elastin and collagen synthesis in the pathogenesis of monocrotaline-induced pulmonary hypertension. *Lab Invest* 1988;58:184–194
7. Todorovich L, Johnson D, Ranger P, Keeley F, Rabinovitch M: Contribution of elastin and collagen to the pathogenesis of monocrotaline-induced pulmonary hypertension (abstract). *Fed Proc* 1986;45:696
8. Rosenberg H, Rabinovitch M: Endothelial injury and vascular reactivity in the pathogenesis of monocrotaline pulmonary hypertension. *Am J Physiol* 1988;255:H1484–H1491
9. Kerr JS, Riley DJ, Frank MM, Trelstad RI, Frankel HM: Reduction of chronic hypoxic pulmonary hypertension in the rat by β-aminopropionitrile. *J Appl Physiol* 1984;57:1760–1766
10. Molteni A, Ward WF, Ts'ao C, Solliday NH, Dunne M: Monocrotaline-induced pulmonary fibrosis in rats: Amelioration by captopril and penicillamine. *Proc Soc Exp Biol Med* 1985;180:112–120
11. Nakao A, Partis RA, Jung GP, Mueller RA: SC-39026, a specific human neutrophil elastase inhibitor. *Biochem Biophys Res Commun* 1987;147:666–674
12. Mainardi CL, Dixit SN, Kang AH: Degradation of type IV collagen by a proteinase isolated from human polymorphonuclear leukocyte granules. *J Biol Chem* 1980;255:5435–5441
13. Mecham RP, Madaras JG, Senior RM: Extracellular matrix specific induction of elastogenic differentiation and maintenance of phenotypic stability in bovine ligamentum fibroblasts. *J Cell Biol* 1984;98:1804–1812
14. Wren FE, Schor AM, Schor SL, Grant ME: Modulation of smooth muscle cell behaviour by platelet derived factors and the extracellular matrix. *J Cell Physiol* 1986;127:297–302
15. Faris B, Toselli P, Kispert J, Wolfe BL, Pratt CA, Mogayzel PJ Jr, Fransblau C: Elastase effect on the extracellular matrix of rat aortic smooth muscle cells in culture. *Exp Mol Pathol* 1986;45:105–117
16. Czer GT, Marsh J, Konopka R, Moser KM: Low-dose PGI_2 prevents monocrotaline-induced thromboxane production and lung injury. *J Appl Physiol* 1986;60:464–471
17. Weeks JR, Jones JA: Routine direct measurement of arterial pressure in unanesthetized rats. *Proc Soc Exp Biol Med* 1960;104:646–648
18. Rabinovitch M, Konstam MA, Gamble WJ, Papanicolaou N, Aronovitz MJ, Treves S, Reid L: Changes in pulmonary blood flow affect vascular response to chronic hypoxia in rats. *Circ Res* 1983;52:432–441

19. Herget J, Palecek F: Pulmonary arterial blood pressure in closed chest rats. Changes after catecholamines, histamine and serotonin. *Arch Int Pharmacodyn* 1972;198:107–117
20. Meyrick B, Gamble W, Reid L: Development of *crotalaria* pulmonary hypertension: Hemodynamic and structural study. *Am J Physiol* 1980;239:H692–702
21. Fulton RM, Hutchinson EC, Jones A: Ventricular weight in cardiac hypertrophy. *Br Heart J* 1952;14:413–420
22. Duncan DB: T tests and intervals for comparisons suggested by the data. *Biometrics* 1975;31:339–359
23. Ghodsi F, Will JA: Changes in pulmonary structure and function induced by monocrotaline intoxication. *Am J Physiol* 1981;240:H149–H155
24. Ward A, Molteni A, Ts'ao C, Solliday N: Monocrotaline pneumotoxicity in mice (abstract). *Fed Proc* 1987;46:994
25. Yamada E, Hazma F, Amano S, Sasahara M, Kataoka H: Elastase, collagenase and cathepsin E activities in the aortas of spontaneously hypertensive and renal hypertensive rats. *Exp Mol Pathol* 1986;44:147–156
26. Hornebeck W, Brechemier D, Bourdillon MC, Robert L: Isolation and partial characterization of an elastase-like protease from rat aorta smooth muscle cells. Possible role in the regulation of elastin synthesis. *Connect Tissue Res* 1981; 8:245–249
27. James HL, James PL, Painter RG, Zahler-Bentz K, Cohen AB: Subcellular localization of platelet elastase and its retention during the release reaction. *Semin Thromb Hemost* 1986;12:250–252
28. Kornecki E, Ehrlich YH, DeMars DD, Lenox RH: Exposure of fibrinogen receptors in human platelets by surface proteolysis with elastase. *J Clin Invest* 1986;77:750–756
29. Sugita T, Stenmark KR, Wagner WW, Henson JE, Hyers TM, Reeves JT: Abnormal alveolar cells in monocrotaline-induced pulmonary hypertension. *Exp Lung Res* 1983; 5:201–215
30. Banda MJ, Werb A: Mouse macrophage elastase. Purification and characterization as a metalloproteinase. *Biochem J* 1981;193:589–605
31. Kay JM, Keane PM, Suyama KL, Gauthier D: Angiotensin converting enzyme activity and evolution of pulmonary vascular disease in rats with monocrotaline pulmonary hypertension. *Thorax* 1982;37:88–96
32. Molteni A, Ward WF, Ts'Ao C, Port CD, Solliday NH: Monocrotaline-induced pulmonary endothelial dysfunction in rats. *Proc Soc Exp Biol Med* 1984;176:88–94

KEY WORDS • pulmonary hypertension • elastase • elastin • vascular smooth muscle • cell differentiation